Development 135, 1439-1449 (2008) doi:10.1242/dev.012849

RNA interference screening in *Drosophila* primary cells for genes involved in muscle assembly and maintenance

Jianwu Bai[1,*], Richard Binari[1,2], Jian-Quan Ni[1,2], Marina Vijayakanthan[1], Hong-Sheng Li[3] and Norbert Perrimon[1,2,*]

To facilitate the genetic analysis of muscle assembly and maintenance, we have developed a method for efficient RNA interference (RNAi) in *Drosophila* primary cells using double-stranded RNAs (dsRNAs). First, using molecular markers, we confirm and extend the observation that myogenesis in primary cultures derived from *Drosophila* embryonic cells follows the same developmental course as that seen in vivo. Second, we apply this approach to analyze 28 *Drosophila* homologs of human muscle disease genes and find that 19 of them, when disrupted, lead to abnormal muscle phenotypes in primary culture. Third, from an RNAi screen of 1140 genes chosen at random, we identify 49 involved in late muscle differentiation. We validate our approach with the in vivo analyses of three genes. We find that *Fermitin 1* and *Fermitin 2*, which are involved in integrin-containing adhesion structures, act in a partially redundant manner to maintain muscle integrity. In addition, we characterize *CG2165*, which encodes a plasma membrane Ca^{2+}-ATPase, and show that it plays an important role in maintaining muscle integrity. Finally, we discuss how *Drosophila* primary cells can be manipulated to develop cell-based assays to model human diseases for RNAi and small-molecule screens.

KEY WORDS: *Drosophila*, Myogenesis, RNAi, Primary cells, Muscle assembly, Human diseases

INTRODUCTION

Drosophila is an excellent model system in which to study muscle development. As in vertebrates, myogenesis occurs in two distinct phases (Nongthomba et al., 2004): (1) acquisition of myoblast cell fate and cell fusion that results in the formation of syncytial myotubes (Bate, 1990); and (2) assembly and maturation of myofibrils (Vigoreaux, 2001). Genetic analysis of naturally occurring and experimentally induced mutants has proven to be an excellent approach to study muscle development. In particular, studies in the *Drosophila* embryo have provided many insights into both the differentiation program of the myogenic pathway and myoblast fusion, illustrating the remarkable conservation of many aspects of myogenesis between flies and vertebrates (Baylies et al., 1998; Chen and Olson, 2004). However, genetic analyses of myofibril assembly have been limited because the functional disruption of genes involved in this process may not allow development to proceed to late larval stages, at which phenotypes are readily discernible (Bernstein et al., 1993). Furthermore, because muscles are multinucleate, screens based on the generation of mutant clones in late larval stages cannot be easily performed. Thus, genetic screens in *Drosophila* have been limited mostly to the identification of a few viable mutations in some major myofibrillar components, such as Indirect flight muscle (IFM) actin (Actin 88F) and Tropomyosin (Vigoreaux, 2001).

Owing to limitations in the use of traditional genetic screens to study muscle biology, we set out to establish a cell-based approach to identify genes involved in the regulation of myofibril assembly using RNA interference (RNAi). In principle, the use of an RNAi-based method could overcome the limitations discussed above, and would allow the examination of myofibril organization at a cellular level. As none of the existing *Drosophila* cell lines we examined is, or could be, transformed into myogenic cells capable of differentiating into mature muscles with organized myofibril structures (J.B., unpublished), we investigated whether muscle cells prepared from primary cells could replace cell lines.

Myogenesis in primary cultures has been used to study muscle biology in both normal and mutant animals (Donady and Seecof, 1972; Volk et al., 1990), and has contributed significantly to our understanding of muscle assembly and maintenance. As earlier studies were largely based on muscle-specific morphological features, such as multiple nuclei in primary myotubes, as well as on myofibril structures observed using light and/or electron microscopy (Bernstein et al., 1978; Echalier, 1997), we set out to confirm and extend previous analyses by following myogenesis in primary culture using muscle-specific molecular markers. We developed conditions for RNAi by culturing cells in the presence of double-stranded RNAs (dsRNAs), and used it to identify genes involved in muscle maintenance and integrity. We validated our approach with in vivo analyses of three genes. We find that *Fermitin 1* and *Fermitin 2*, which are involved in integrin-containing adhesion structures, act in a partially redundant manner to maintain muscle integrity. In addition, we characterized *CG2165*, which encodes a plasma membrane Ca^{2+}-ATPase (PMCA), and showed that it plays an important role in maintaining muscle integrity. Finally, we discuss how *Drosophila* primary cells can be manipulated to develop cell-based assays to model human diseases for RNAi and small-molecule screens.

MATERIALS AND METHODS

Drosophila genetics

Drosophila strains used in this study are *Dmef2-Gal4* (Ranganavakulu et al., 1996), *D42-Gal4* (Gustafson and Boulianne, 1996), *Hand-Gal4* (Arbrecht et al., 2006), *rp298-lacZ* (Ruiz-Gomez et al., 2000), *UAS-mitoGFP* (Cox and Spradling, 2003), *UAS-2EGFP* (Halfon et al., 2002), *G053* (SLS-GFP) (Morin et al., 2001), *MHC-τGFP* (Chen and Olson, 2001) and *5053A* (Mandal et al., 2004). w^{1118} was used as a wild-type strain.

[1]Department of Genetics and [2]Howard Hughes Medical Institute, Harvard Medical School, 77 Avenue Louis Pasteur, Boston, MA 02115, USA. [3]Department of Neurobiology, University of Massachusetts Medical School, Worcester, MA 01605, USA.

*Authors for correspondence (e-mails: jbai@genetics.med.harvard.edu; perrimon@receptor.med.harvard.edu)

Accepted 11 February 2008

Embryonic primary cell cultures

Embryonic primary cell cultures were established as described previously (Bernstein et al., 1978). Briefly, eggs were collected on molasses plates streaked with killed yeast paste for 2 hours and incubated for an additional 4 hours at 25°C. Embryos were dechorionated in 50% bleach for 3 minutes, rinsed thoroughly with 70% ethanol and sterilized water, and dissociated into a cell suspension using Dounce homogenizers (VWR Scientific, Seattle, WA) (7 ml for smaller scale, 40 ml or 100 ml for larger scale preparations) in Shields and Sang M3 medium (Sigma). Cell suspensions were spun once at 40 ***g*** for 10 minutes to pellet tissue debris, large cell clumps and vitelline membranes. The supernatant was then transferred to a fresh tube and spun at 360 ***g*** for 10 minutes to pellet the cells. Cells were washed once and resuspended in primary cell medium [10% heat-inactivated fetal bovine serum (JRH Biosciences), 10 mU/ml bovine insulin (Sigma) in M3 medium]. Cells were seeded and grown in 384-well optically clear plastic plates (Costar) at 1.7-2.5×10^5 cells/cm^2 (no extra coating steps required).

Immunofluorescence microscopy and western blotting

Protocols for dissection of late embryos or first instar larvae, and for the staining of dissected tissues and primary cells, are described in detail elsewhere (Bai et al., 2007). Primary antibodies used were: rabbit anti-Dmef2 (Bour et al., 1995), rabbit anti-Lmd (Duan et al., 2001), mouse anti-Mhc and anti-α-Actinin (Actn) (from Dr J. Saide, Boston University, Boston, MA), and rat anti-Tropomyosin (The Babraham Institute, Cambridge, UK). Secondary antibodies were from Jackson Laboratories.

For western blotting, early first instar larvae (30 hours AEL at 25°C) were homogenized in sampling buffer, and whole-body protein extracts (equivalent to five larvae) were subjected to western blotting and probed with anti-*Drosophila* PMCA (Lnenicka et al., 2006) and mouse anti-α-tubulin (Sigma).

Primary cell RNAi and staining

Our protocol for a primary cell RNAi screen for muscle genes is outlined in Fig. 4A. Briefly, primary cells were isolated from post-gastrula embryos (4-6 hours AEL at 25°C), and seeded in 384-well plates containing different individual dsRNAs in each well using a MultiDrop (Thermo Scientific) liquid dispenser at ~3-4×10^4 cells (in 10 μl) per well. After 22 hours in serum-free M3 medium at 18°C, the MultiDrop was used to add to each well 30 μl of serum-containing medium to bring the final concentration of fetal calf serum to 10%. Primary cells were then cultured for an additional 10-11 days at 18°C before fixation with 4% formaldehyde. Cells were stained overnight at 4°C with phalloidin Alexa Fluor 568 (Molecular Probes; 1:2000) and DAPI (Sigma, 1:5000) in PBTB (PBS, 0.1% Triton X-100, 1% BSA), washed once in PBS and left in PBS containing 0.02% NaN_3.

RNAi screen and image annotation

dsRNAs were obtained from the *Drosophila* RNAi Screening Center (DRSC) at Harvard Medical School; details of dsRNA synthesis and the amplicons used in this study can be found at http://flyrnai.org/. Because primary myocytes were relatively large and were in general distributed sparsely and randomly in the well, rather than capturing the images using an automated microscope, we visually inspected the wells using an inverted microscope and then imaged those wells containing cells with abnormal muscle phenotypes. Phenotypes were classified into one of four categories (see Results), and the severity of the phenotypes was defined by the percentage of mutant muscles in the well: 'severe' describes cases in which over 80% of muscles showed a certain phenotype, whereas 'medium' describes cases in which ~50% showed a mutant phenotype.

To address the issue of off-targets associated with dsRNAs (Kulkarni et al., 2006; Ma et al., 2006), independent dsRNAs were used. For a list of those genes whose RNAi phenotypes were reproducibly observed with an independent second set of amplicons, see Table S2 in the supplementary material; for the IDs of the amplicons used for generating dsRNAs targeting these genes, see Table S3 in the supplementary material. For a list of all the genes screened in this study, see Table S4 in the supplementary material.

Embryo RNAi injection, in situ hybridization and confocal microscopy

Embryonic in situ hybridizations were performed as described (Hauptmann and Gerster, 2000). dsRNAs (prepared as described at http://flyrnai.org/) were injected at 2 μg/μl into *MHC-τGFP* embryos through their mid-ventral side according to a standard embryo injection protocol (Kennerdell and Carthew, 1998). Injected embryos were aged at 25°C for 20 hours and then analyzed with a Leica LSM NT confocal microscope.

Establishment of transgenic RNAi lines targeting *CG2165*

The snap-back hairpin construct targeting *CG2165* was made in the VALIUM (Vermilion-AttB-Loxp-Intron-UAS-MCS) vector (forward primer, 5′-GTCTAGAGACATGAGGGCACTTTGGAG-3′; reverse primer, 5′-AGAATTCCATTGCTATCACGAATACGCC-3′), and *UAS-CG2165 hp* transgenic flies were generated as described by Ni et al. (Ni et al., 2008).

Single-cell $[Ca^{2+}]_i$ imaging

Primary muscles used for single-cell $[Ca^{2+}]_i$ imaging were derived from cells dissociated from wild-type control embryos and those carrying *UAS-drc2/+; Dmef2-Gal4/UAS-CG2165 hp*, and were cultured in complete media in 8-well cover-glass chamber slides coated with human vitronectin (Chemicon) at 25°C for 3 days. Primary cells were washed twice with low-calcium Ringer solution (150 mM NaCl, 4 mM $MgCl_2$, 5 mM KCl, 0.5 mM $CaCl_2$, 10 mM HEPES, pH 7.2), loaded with Fura PE 3 [5 μM Fura PE 3-AM (Sigma F0918), 0.02% pluronic acid (Molecular Probes) in low-calcium Ringer solution at room temperature]. After a 90 minute incubation, cells were washed twice with Ringer solution, followed by a 30 minute incubation for further dye cleavage. The loaded cells were examined using a Nikon inverted epifluorescence microscope and a 100× oil-immersion lens. Only primary muscles with well-spread morphology were subjected to calcium ratio imaging analysis, with the excitation beams at 340 and 380 nm and the emission wavelength at greater than 510 nm. Images were acquired with Ratiotool software (Inovision, Raleigh, NC). $[Ca^{2+}]_i$ was calculated as described by Grynkiewicz et al. (Grynkiewicz et al., 1985): $[Ca^{2+}]_i = Kd \times [R - R\text{min}]/[R\text{max} - R]$, where Kd is the Fura PE 3 dissociation constant for calcium (251 nM) (Kermode et al., 1990), R is the ratio of intensities at 340 and 380 nm, and Rmin and Rmax are the R values at 0 and saturating levels of calcium (10 mM), respectively.

RESULTS

Myogenesis in primary cell cultures derived from *Drosophila* embryos

To characterize *Drosophila* myogenesis in vivo, primary cells were dissociated from gastrulating embryos following a mass homogenization (see Materials and methods). Embryos were collected at stage 10 or 11 [4-6 hours after egg laying (AEL) at 25°C] when myoblast cell fate is already specified but before fusion is initiated (Bate, 1993). To characterize the freshly dissociated cells, we fixed and stained them for a number of myoblast-specific markers (Fig. 1A-F). In these cultures, based on the number of cells expressing the myogenic transcription factor Dmef2 (*Drosophila* Mef2) (Bour et al., 1995), myoblasts represented 15±2% (±s.e.m., from five independent preparations) of the cell population. In addition, both founder cells and fusion-competent cells could be easily distinguished by the expression of specific markers, such as *rp298-lacZ* for founder cells (Ruiz-Gomez et al., 2000) (Fig. 1D-F), and Lame duck (Lmd) for fusion-competent cells (Duan et al., 2001) (Fig. 1F). Consistent with the observation that the expression of muscle Myosin begins at stage 13 when myoblast fusion has already occurred (Bate, 1993), we failed to detect any expression of muscle Myosin heavy chain (Mhc) in the newly isolated cells (data not shown).

Since fusion is a significant event in myogenic cell differentiation, we confirmed the observation that fusion occurs in culture. When cells originating from *Dmef2-Gal4* and *UAS-2EGFP* embryos,

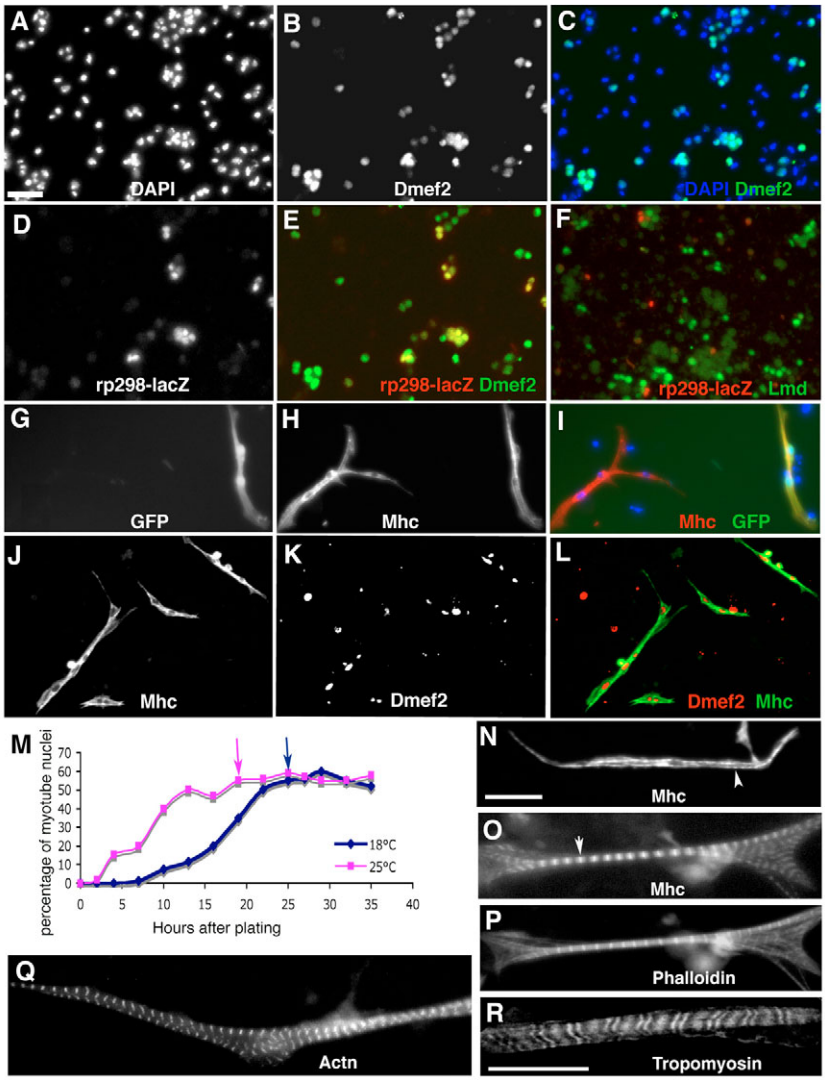

Fig. 1. Myogenesis in primary cultures derived from *Drosophila* embryos. (**A-F**) Fluorescence micrographs of freshly dissociated cells obtained from *Drosophila* gastrulating embryos carrying *rp298-lacZ* immediately following plating. Cells are stained using DAPI for nuclei (A, and blue in C), and antibodies targeting Dmef2 (B, and green in C,E), β-galactosidase (D, and red in E,F) and Lmd (green in F). (**G-I**) Primary cells derived from *Dmef2-Gal4* embryos were mixed with those from *UAS-2EGFP* and allowed to develop for 48 hours at 18°C in culture. The GFP-positive myotube (G, and green in I) resulted from fusion of cells supplied by two genetically different embryos, and the GFP-negative one is most likely derived from the fusion of cells from two genetically identical embryos. Both myotubes expressed Mhc (H, and red in I). (**J-L**) Multinucleated myotubes are identified by staining for Mhc (J, and green in L) and for Dmef2 (K, and red in L). Note that not all Dmef2-positive nuclei are found in myotubes. The percentage of myotube nuclei among the total number of Dmef2-positive nuclei was used as an indication of the amount of fusion. (**M**) Time-course of myoblast fusion at 18°C and 25°C. Primary cell cultures were fixed and stained for Dmef2, Mhc or Actin at the times indicated. The number of Dmef2-positive nuclei was counted using Autoscope and Metamorph software. The number of nuclei in the myotubes was determined manually. The percentage of myotube nuclei was estimated by the number of myotube nuclei among the total Dmef2-positive nuclei, and used as an indication of the extent of myoblast fusion. Each point represents the average results of two or three trials. Arrows point to the time when fusion is nearly complete (pink for 25°C and blue for 18°C). (**N**) Fluorescence micrograph of a primary myotube from a 2-day culture at 18°C stained for Mhc. The white arrowhead points to the immature myofibril that formed along the side of the myotube. (**O-R**) Primary myotubes from 11-day cultures at 18°C, stained for Mhc (O), Actin (as detected using phalloidin) (P), Actn (Q) and Tropomyosin (R). The short arrow in O indicates the bundled myofibrils. Scale bars: 20 μm, in A for A-L and in N for N-Q.

respectively, were mixed, we detected GFP expression in a fraction of multinucleated myotubes (Fig. 1G-I and see Movie 1 in the supplementary material). These GFP-expressing cells indicated the fusion of myoblasts supplied by two different classes of embryos, one expressing *Gal4* and one carrying *UAS-GFP*. We next followed the time-course of myoblast fusion in cultures at 25°C and 18°C (Fig. 1J-M). We found that fusion began ~2 hours after plating, and became rare after 16 hours at 25°C. However, fusion takes place at a much slower pace at 18°C (J.B., N.P., J. Lu and A. Michelson, unpublished), as it initiated at ~7 hours after plating and could last for another 18 hours. Cell density had no significant effect on the fusion rate, although it did affect subsequent muscle differentiation, which probably required myotubes to spread well in culture (data not shown). We further determined the number of nuclei in myotubes in 2-day-old cultures following plating, when fusion is essentially complete at both temperatures. In contrast to myotubes

in vivo that have an average of 10-11 nuclei by the completion of fusion (Bate, 1993), the number of nuclei per myotube in culture was 3.48±0.5 (range from 2 to 15), with 2-5 nuclei seen most commonly (scored in ~100 myotubes in three independent cultures); for representative examples, see Fig. 1L. As visceral muscles have fewer fusions in vivo than somatic muscles, we investigated whether the primary myotubes in our cultures might be primarily of visceral muscle origin by examining the cultures for several visceral muscle markers, including *Hand-Gal4*, *UAS-2EGFP* (circular visceral and cardiac muscles) (Arbrecht et al., 2006), and *5053A*, *UAS-2EGFP* (longitudinal visceral muscles) (Mandal et al., 2004). Only very few myotubes (~2%) were found to co-express GFP in primary cultures derived from embryos carrying *5053A*, *UAS-2EGFP* (data not shown) and ~20% were labeled with the *Hand-Gal4*, *UAS-2EGFP* combination (see Fig. S1 in the supplementary material), indicating that most primary myotubes in culture are derived from somatic muscle cells. Thus, we speculate that the fewer fusions observed in the primary culture might result from the dispersed distribution of myoblasts among other cell types. Relatively pure myoblast preparations may give rise to myotubes having more nuclei (Storti et al., 1978).

Next, we followed the assembly and maturation of myofibrils by staining cells in culture for Actin and Mhc at different time points. Thin and thick filaments were detected as regular patterns at 13 hours after plating at 25°C or when grown for 22 hours at 18°C (data not shown). Later, they aligned and began to organize into parallel bundles and striation became clearly visible at around 19 hours at 25°C or 29 hours at 18°C. These newly formed myofibrils were thin and often found along the lateral sides of myotubes (Fig. 1N). Within ~5-7 days at 25°C (or 10-13 days at 18°C), these strip-like myotubes became mature and stable, with much thicker and more bundled myofibrils (Fig. 1O-R), indicating that the maturation process is achieved by adding more myofibrils laterally. Approximately 52% (52±0.8%) of the myoblasts initially plated in the culture were able to survive to the later stage and developed a fiber-like morphology. About 75% of those with a fiber-like morphology had well-defined striated thick and thin filaments, as revealed by staining for muscle markers, such as Mhc, Actin, Tropomyosin and Actn (Fig. 1O-R). We estimated that ~48% of myoblasts initially plated died after being cultured for an extended period of time. The maximum length of sarcomeres in mature myofibrils was ~8 μm, comparable to that in late L3 body-wall muscles. The average length (6±0.73 μm) of the recognizable sarcomeres remained unchanged during in vivo maturation of the primary muscles. Importantly, some of these primary muscle cells were actively contracting in culture, indicating that they were fully functional (see Movies 1, 2 in the supplementary material). In addition, we found that primary muscles could be detected on the basis of their phalloidin staining alone, as other cell types such as neurons did not display strong phalloidin staining (Fig. 2A-D). Thus, by simply monitoring the strong Actin staining of muscle cells with phalloidin, we can follow myotube differentiation into organized branch-like shapes with a striated structure, and distinguish them from other cell types, including those known for their roles in regulating muscle function in vivo, such as neurons (Fig. 2E-H) and tendon cells (data not shown) (Tucker et al., 2004).

RNAi is an effective method to perturb gene activity in primary cells

Because the use of RNAi in *Drosophila* primary cells had not been previously reported when we started this work, we conducted experiments to establish whether the addition of dsRNAs to primary cells could elicit a robust gene interference response. As serum starvation can significantly facilitate effective cellular uptake of dsRNAs from the medium (Clemens et al., 2000), we

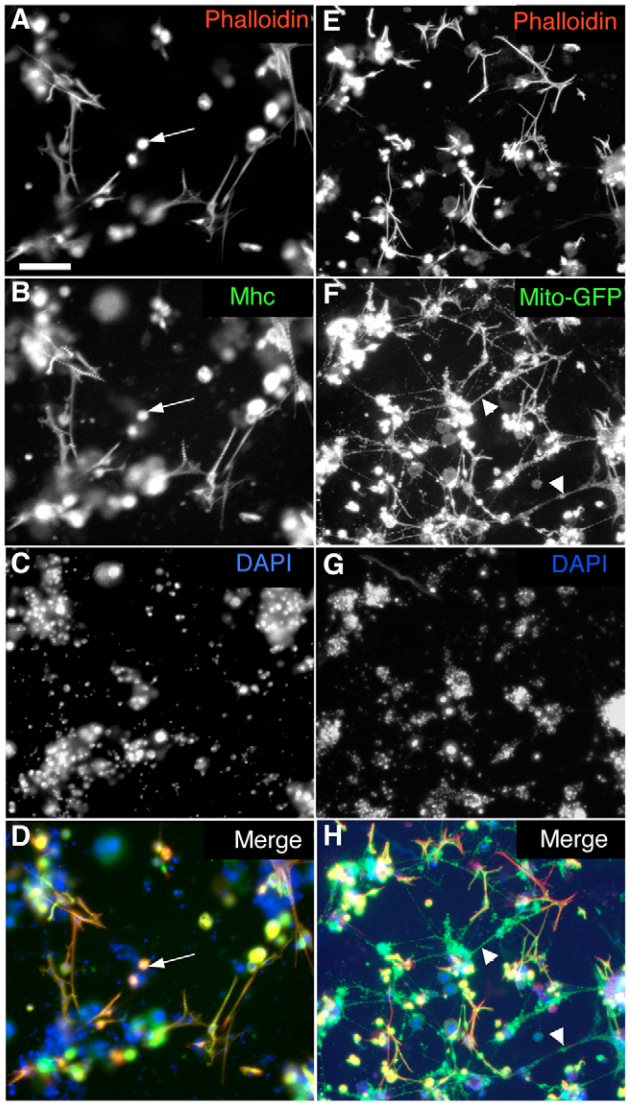

Fig. 2. Primary cultures derived from *Drosophila* embryonic cells contain a mixture of different cell populations that include muscles and neurons. (**A-D**) Primary myotubes strongly stained by phalloidin (A, red in the merged image in D) are all stained for Mhc (B, green in the merged image in D). Note that other cell types whose nuclei are revealed by DAPI (C) are faintly visible by phalloidin staining. As myotubes mature they become more contractile, some detach from the tissue culture surface, and are seen as round muscles (arrows in A,B,D). (**E-H**) Primary cells were isolated from *Dmef2-Gal4*, *D42-Gal4*, *UAS-mito-GFP* embryos in which *Dmef2-Gal4* and *D42-Gal4* drive expression of mito-GFP, a mitochondrial marker transgene that fuses the mitochondrial targeting signal to the N-terminus of EGFP, in muscles and motoneurons, respectively. Muscle structure is visualized by phalloidin staining of Actin (E, red in the merged image in H), and neurons can be seen in F (green in the merged image in H) as they stain strongly with mito-GFP but not phalloidin (triangles in F,H). In addition to neurons and muscles, other cells are present in the culture, as revealed by the staining with DAPI (G, blue in the merged image in H). In H, muscles are shown in red and yellow, neurons and their extensions in green only. Scale bar: 50 μm.

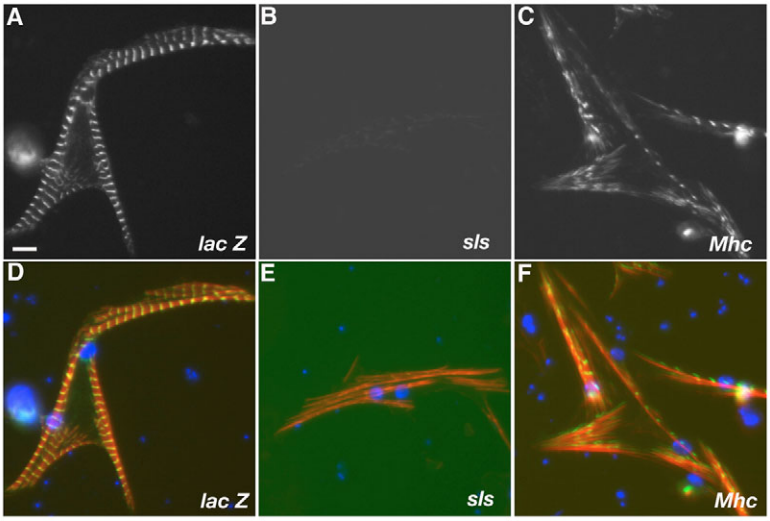

Fig. 3. Gene-specific RNAi effects in primary cells. Primary cells were isolated from *G053 Drosophila* embryos expressing the SLS-GFP fusion protein and were treated with dsRNAs targeting *lacZ* (**A**,**D**), *sls* (**B**,**E**) and *Mhc* (**C**,**F**). SLS-GFP expression was detected by GFP (A-C, green in D-F). Muscle structure was revealed by SLS-GFP in green, phalloidin staining of Actin in red, and DAPI staining of nuclei in blue (D,E,F). Scale bar: 20 μm.

first determined how it would affect myogenesis in culture. Although myoblast fusion did not require a serum supplement and could proceed to completion in its absence (see Fig. S2 in the supplementary material), myofibrils rarely formed myotubes without serum, probably owing to a lack of stimulatory factors required for their efficient assembly (Volk et al., 1990) (data not shown). Thus, we chose to starve cells for 22 hours at 18°C, when myofibril assembly initiates, and then added serum back to the cultures. This treatment did not perturb the time-course of myogenesis (see Fig. S2 in the supplementary material). Furthermore, we found that simple bathing of *Drosophila* primary cells in serum-free medium containing dsRNAs for 22 hours, followed by incubation in serum-containing medium at 18°C, was sufficient to elicit a robust and specific RNAi response. Primary cells were prepared from embyos of line *G053*, a homozygous viable enhancer-trap line carrying an in-frame insertion of *GFP* in the gene *sallimus* (*sls*), which encodes a sarcomeric protein related to vertebrate titin (Morin et al., 2001). Treatment of primary cells using control dsRNA targeting *lacZ* does not affect myofibril structure or change SLS-GFP expression (Fig. 3A,D). However, *sls* dsRNA abrogated the expression of the SLS-GFP and disrupted myofibril structure (Fig. 3B,E), whereas treatment with a dsRNA against *Mhc* interfered with its striated pattern (Fig. 3F) but did not affect SLS-GFP expression (Fig. 3C). In both cases, the RNAi knock-down was observed in 90% of existing muscle cells. In addition, we did not observe any difference in the RNAi effects within myotubes containing different numbers of nuclei, indicating that myotubes derived from more fusion events are as sensitive to RNAi treatment as those derived from fewer fusion events. Importantly, both the *sls* and *Mhc* RNAi phenotypes (Fig. 3E,F) faithfully mimicked those found in vivo in *sls* and *Mhc* mutant muscles, respectively (O'Donnell and Bernstein, 1988; Zhang et al., 2000). Furthermore, the use of SLS-GFP allowed us to follow the RNAi effect in live myotubes, which we could detect as early as 2 days after serum addition. At this time, the expression of SLS-GFP was hardly detectable in live myotubes in wells containing dsRNAs targeting *sls*, whereas live myotubes in control wells started to show organized SLS-GFP expression and myofibril structure (data not shown). The RNAi effect was more robust after 8-11 days (Fig. 3), when the expression of muscle proteins such as Actin, Myosin and SLS-GFP became stronger, and the myotubes more differentiated.

RNAi phenotypes of *Drosophila* genes that are homologous to human genes associated with muscle diseases

Using the approach outlined in Fig. 4A, we analyzed the RNAi phenotypes in primary muscle cells of *Drosophila* genes that are homologous to human genes associated with muscle diseases (see Table S1 in the supplementary material). We attempted to analyze the functional role of these *Drosophila* homologs of human disease genes in myofibril assembly and maintenance of muscle integrity. Among the 28 genes that we analyzed, 19 of them, when disrupted by RNAi, led to various muscle phenotypes (see Table S1 in the supplementary material) that fell into four distinct categories. In Class I, over 70% of myotubes failed to extend and usually rounded up, whereas neurons differentiated well in the same culture (Fig. 4C and see Fig. S3 in the supplementary material). Rounded-up muscles might indicate that the muscles failed to spread or maintain spreading on the surface of plates. Both *multiple edematous wings* (*mew*) and *myospheroid* (*mys*), which are the orthologs of the human integrin alpha- and beta-subunit genes, respectively, belong to this class (Fig. 4C and data not shown), indicating that muscle spreading on the plate requires integrin-mediated adhesion (Estrada et al., 2007; Volk et al., 1990). Phenotypes in Classes II and III consisted of disrupted sarcomeric structures with severely compromised or no striation, as detected by phalloidin staining (Fig. 4D,E). Actin filaments of Class II muscles usually had no discernible striations, whereas Myosin filaments still showed a striated pattern. Moreover, the myofibril length of Class II muscles was in general shorter than that of wild-type muscles. A representative example of this class is the *sls* gene (Fig. 3E, Fig. 4D). The ratio between the length and width of the myofibrils in *sls* RNAi muscles was ~7.5 per nucleus, which was much less than that of wild-type muscles (~21 per nucleus). In Class III muscles, both Actin and Myosin filaments lacked striation, and Actin filaments appeared more spread out (Fig. 4E). Genes in this class have been implicated in the regulation of Myosin function [*Mhc* and *Myosin light chain 2* (*Mlc2*)], or serve to mediate interactions between thin and thick filaments [*wings up A* (*wup A*), *upheld* (*up*) and *bent* (*bt*) (Vigoreaux, 2001)]. Their RNAi phenotypes demonstrate that both thick filaments and the interactions between thin and thick filaments are essential for sarcomeric order and periodicity (Clark et al., 2002). Finally, in Class IV, muscles had normal myofibril structures, but were thinner or shorter than in the wild type (Fig.

4F). dsRNAs simultaneously targeting all Actin isoforms led to this phenotype (Fig. 4F), probably reflecting the temporal effect of knocking-down Actin by RNAi after myoblast fusion. Since Actin is essential for building myofibrils, this phenotype might result from an arrest in myofibril assembly owing to a lack of available Actin monomers.

Strikingly, dsRNAs targeting *Drosophila* homologs of human dystrophin complex genes did not cause any obvious muscle phenotypes (see Table S1 in the supplementary material, and data not shown). A potential explanation is that these genes, mutations in which are associated with various types of human muscular dystrophies, are required for maintaining muscle strength and integrity (Dalkilic and Kunkel, 2003) (see Table S1 in the supplementary material). This is in contrast to congenital myopathies and cardiomyopathies, which are usually caused by the disruption of genes encoding sarcomeric components (Bornemann and Goebel, 2001; Clarkson et al., 2004; Seidman and Seidman, 2001) (see Table S1 in the supplementary material). Therefore, it is possible that muscles in culture do not experience the same mechanical stress as they do in vivo. In summary, our study of *Drosophila* genes homologous to known human muscle disease genes demonstrates the potential of RNAi in *Drosophila* primary muscles to analyze the loss-of-function of these genes, which might provide clues to the further understanding of the mechanism underlying human muscle diseases.

A screen for new genes involved in muscle assembly and maintenance

To estimate the number of genes in the *Drosophila* genome that are involved in muscle assembly, we analyzed a random set of dsRNAs targeting 1140 genes. Among these, 49 genes were confirmed to be associated with distinctive and reproducible phenotypes (four belong to Class I, 28 to Class II, 5 to Class III and 12 to Class IV) (see Table S2 in the supplementary material). Interestingly, 22 of the 49 genes (45%) have not been previously reported to be involved in late muscle differentiation, and 27 out of 49 (55%) are either expressed or putatively enriched in the mesoderm (either myoblasts and/or muscle tissues) (see Table S2 in the supplementary material). Finally, as these 1140 genes represent ~8% of the *Drosophila* genome (~14,000 genes covered with dsRNAs available in DRSC), we estimate that the total number of candidate genes implicated in muscle differentiation and maintenance (as defined by the morphological criteria used in this study) in a genome-wide screen would be around 580 (~4% of the genome).

In vivo validation by injection of dsRNAs into embryos or transgenic RNAi

We selected three Class I genes for in vivo validation, as the rounded-up muscle phenotype can be easily detected. We chose *Fermitin 1* (*Fit1*) and *Fermitin 2* (*Fit2*) because their function in *Drosophila* muscles had not been previously recognized, and in *C*.

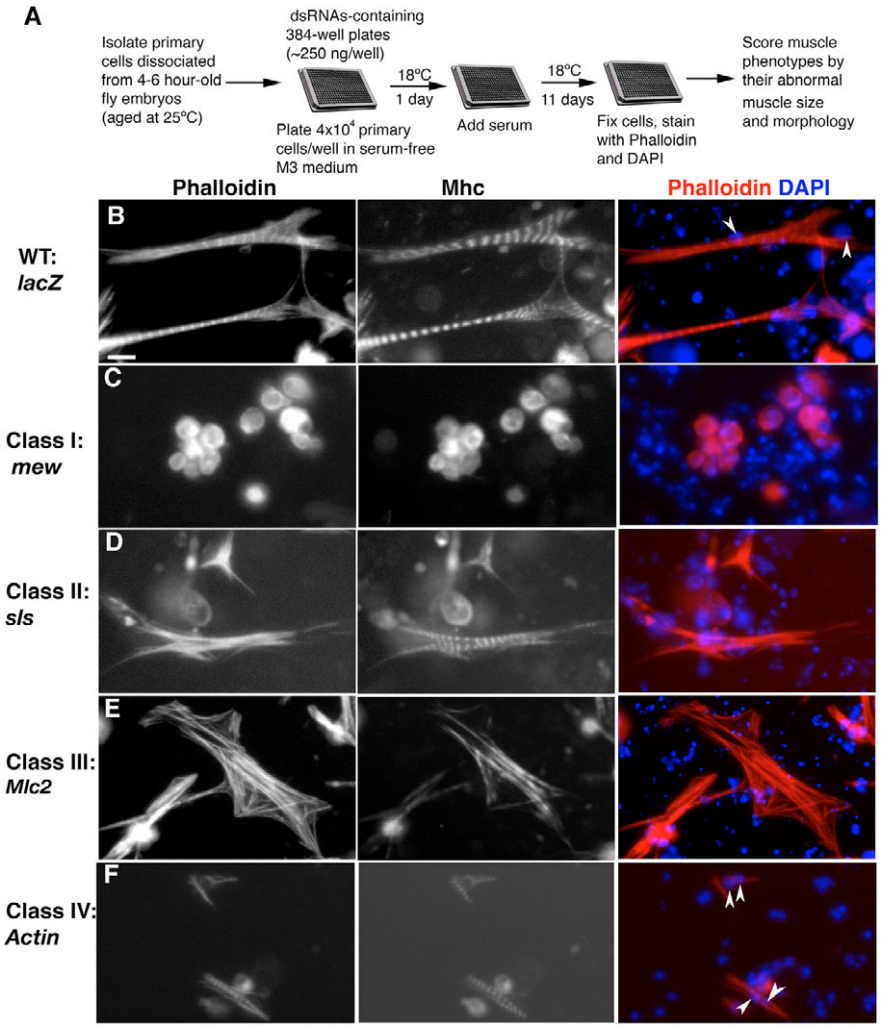

Fig. 4. Phenotypic classes identified from the RNAi screen. (**A**) Protocol for RNAi screening in primary cultures. (**B-F**) Four distinct classes of muscle phenotype were distinguished based on the staining of Actin using phalloidin (left panels, and red in right panels), Mhc (middle panels) and of nuclei with DAPI (blue in right panels). (B) Wild-type control myotubes treated with dsRNAs targeting *lacZ*. (C) Class I (treated with *mew* dsRNAs). (D) Class II (treated with *sls* dsRNAs). (E) Class III (treated with *Mlc2* dsRNAs). (F) Class IV (treated with *Actin* dsRNAs simultaneously targeting all Actin isoforms, including *Act42A*, *Act57B*, *Act5C*, *Act79B*, *Act87E* and *Act88F*). Note that the four phenotypic classes did not result from fewer fusions, as muscles contained the same number of nuclei as controls. Arrowheads point to the nuclei. Scale bar: 15 μm.

elegans the orthologous protein, UNC-112, had been shown to be involved in the assembly of integrin-containing adhesion structures (Rogalski et al., 2000). In our screen, knock-down of *Fit1* and *Fit2* individually by their corresponding dsRNAs only caused partial rounded-up muscle phenotypes, i.e. some muscles rounded up but some with branch-like morphology were still present (see Fig. S3A-C in the supplementary material). However, knock-down of these two genes together led to a complete rounded-up muscle phenotype (see Fig. S3D-F in the supplementary material, compared with wild type in Fig. 2), suggesting that their functions are partially redundant.

To validate this observation in vivo, we first examined *Fit1* and *Fit2* expression during embryogenesis by in situ hybridization. Strikingly, both genes are expressed in the musculature (Fig. 5A-E), in a pattern reminiscent of *mys* (MacKrell et al., 1988). Next, we interfered with the function of these genes by directly injecting dsRNAs against *Fit1* and *Fit2* into embryos. To ensure specificity, we used both negative (*lacZ*) and positive (*mys*) control dsRNAs in our injection. Embryos injected with *lacZ* dsRNAs did not show any discernible phenotype (Fig. 5F), whereas embryos injected with *mys* dsRNAs displayed the expected germ band retraction and round muscle phenotypes (Fig. 5G) (MacKrell et al., 1988). When *Fit1* or *Fit2* dsRNAs were injected alone, we observed that some muscles consistently rounded up (Fig. 5H,I, short arrows), although some did not seem to be affected (Fig. 5H,I, long arrows). However, the vast majority of muscles showed a rounded-up phenotype when embryos were co-injected with both *Fit1* and *Fit2* dsRNAs (Fig. 5J). These results suggest that *Fit1* and *Fit2* have overlapping roles in vivo, a conclusion that has been independently confirmed by a genetic analysis of *Fit1* and *Fit2* mutations (D. Devenport and N. Brown, personal communication).

We also validated *CG2165*, another Class I gene, using a transgenic line carrying a snap-back hairpin construct targeting this gene (see Materials and methods). Although dsRNAs targeting *CG2165* (referred to as *CG2165* RNAi) caused complete rounded-up muscle phenotypes after primary cells were cultured for 11 days at 18°C (Fig. 6D), time-course examination of 4-day and 8-day cultures showed that the majority of *CG2165* RNAi primary muscles were well spread on day 4 of culture (Fig. 6C), but few were found to have elongated morphology on day 8 of culture (Fig. 6E). These results indicated that *CG2165* may not be required for the initial spreading of primary muscles in culture, but is required for maintaining muscle morphology.

CG2165 is located at 102B5-102B5 on the fourth chromosome, and currently there are no available mutations in this gene. *CG2165* is the only gene in the *Drosophila* genome that encodes a plasma membrane Ca^{2+}-ATPase (PMCA), the putative function of which is to extrude calcium from cells, thereby maintaining a low cytosolic calcium concentration ($[Ca^{2+}]_i$) (Gwack et al., 2006). The gene is expressed ubiquitously in all tissues, including muscle (Lnenicka et al., 2006; Roos et al., 2005) (data not shown). The function of PMCA in muscle cells has not been described previously in *Drosophila* or vertebrates. To investigate the function of *Drosophila* PMCA in muscle cells in vivo, we used the *Gal4-UAS* binary system (Brand and Perrimon, 1993) to drive expression of the hairpin construct in muscles using *Dmef2-Gal4* along with the overexpression of Dicer-2 (Dcr-2) [*UAS-Dcr-2/+; Dmef2-Gal4/UAS-CG2165 hp* (referred to as muscle-specific *CG2165* RNAi)]. Dcr-2 was used to increase the RNAi effect (Dietzl et al., 2007), as we have observed the same muscle phenotype with and without Dcr-2 (*Dmef2-Gal4/UAS-CG2165 hp*), although the phenotype is less penetrant without Dcr-2 (data not shown). Moreover, larvae with overexpression of Dcr-2 alone (*UAS-Dcr-2; Dmef2-Gal4*) showed wild-type muscle morphology (Fig. 6H and data not shown). Muscle-specific *CG2165* RNAi significantly reduced the expression of its corresponding protein PMCA (Fig. 6F). Disruption of *CG2165* function did not appear to affect muscle development, as the majority of larvae expressing muscle-specific *CG2165* RNAi hatched (141/200 versus 130/161 observed in *UAS-Dcr-2; Dmef2-Gal4* controls), although all larvae died during early first instar. While still alive, these larvae were sluggish and generally were shorter and appeared hypercontracted

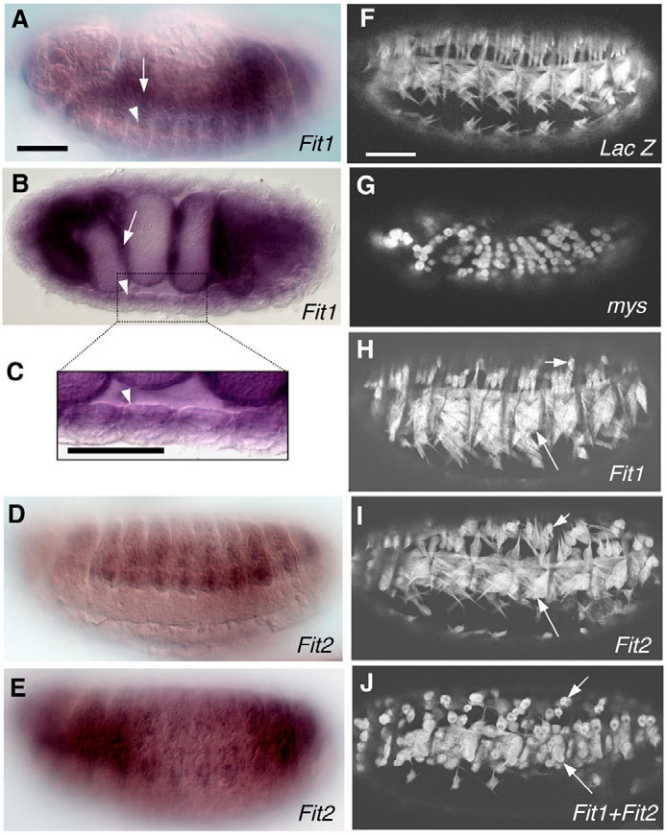

Fig. 5. In vivo validation of *Fit1* and *Fit2* using dsRNA injection. (**A-E**) Micrographs of whole-mount in situ hybridizations of *Drosophila* embryos with Dig-labeled antisense probes specifically targeting *Fit1* (A-C) and *Fit2* (D,E), oriented anterior to the left. (A,D) Lateral view of stage 14 embryos. (B) Dorsal view of a stage 16 embryo focusing on visceral muscle and somatic body wall muscles. (C) High-magnification image showing *Fit1* somatic body wall muscle expression. Arrowhead, somatic body wall muscles; arrow, visceral gut muscles. (E) Lateral view of a stage 16 embryo. (**F-J**) Fluorescence micrographs of stage 17 embryos carrying MHC-τGFP. dsRNAs targeting (F) *lacZ* (2 μg/μl), (G) *mys* (2 μg/μl), (H) *Fit1* (2 μg/μl), (I) *Fit2* (2 μg/μl) and (J) *Fit1* (1 μg/μl) + *Fit2* (1 μg/μl) were injected into MHC-τGFP embryos. MHC-τGFP allows visualization of all somatic muscles, as shown in F, where the embryos were injected with a negative control dsRNA targeting *lacZ* (*n*=67, none showed muscle phenotypes). Note that severely rounded muscles are present in the embryos injected with dsRNAs targeting *mys* (G) (100% penetrance, *n*=87, where *n* is the number of embryos injected) and *Fit1* + *Fit2* (J) (96% penetrance, *n*=150), whereas dsRNAs targeting either *Fit1* (H) or *Fit2* (I) alone only caused some muscles to round up (short arrows in H,I). Long arrows in H-J point to the ventral acute muscles that are still present as fibers in H and I, but round up in J. Scale bars: 50 μm in A for A-E, in F for F-J.

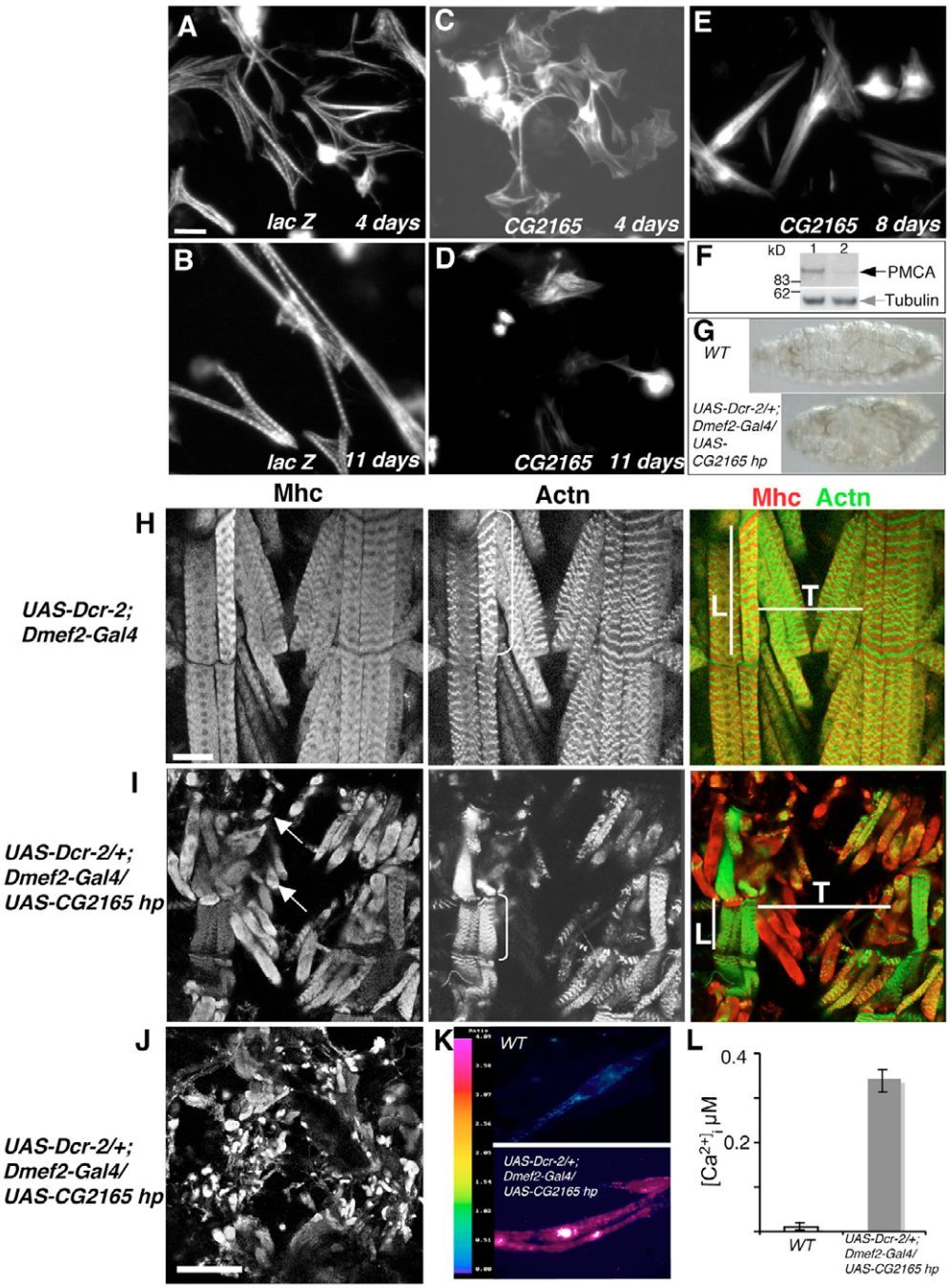

Fig. 6. In vivo validation of *CG2165* using transgenic RNAi. (**A-E**) Wild-type (A,B) and *CG2165* RNAi (C-E) primary muscle phenotypes at 18°C cultured for 4 days (A,C), 8 days (E) and 11 days (B,D), revealed by phalloidin staining for Actin. (**F**) Western blots probed with rabbit anti-*Drosophila* PMCA (top) and mouse anti-tubulin (bottom, as loading controls). Note that the expression of PMCA was significantly reduced in muscle-specific CG2165 RNAi larvae (lane 2) compared with wild type (lane 1). (**G**) Comparison of the body size in wild-type (top) and muscle-specific CG2165 RNAi (bottom) first instar larvae of the same age (30 hours AEL at 25°C). Note the short size and hypercontracted appearance of muscle-specific CG2165 RNAi larvae. (**H**,**I**) Confocal fluorescent micrographs showing the ventral internal muscles of first instar larvae of *UAS-Dcr-2; Dmef2-Gal4* (H) and muscle-specific CG2165 RNAi (I) stained for Mhc and Actn. Arrows in I point to the rounded-up muscles. Note that although both control and muscle-specific CG2165 RNAi VL4 muscles (brackets) contained a comparable number of sarcomeres longitudinally, the length of CG2165 RNAi VL4 muscles is only half that of the wild type (lines labeled L), and thus the sarcomere size was only ~50% of that in wild type. Also note that the transverse distance (T) between two VL4 muscles in the same segment in muscle-specific CG2165 RNAi larvae is much greater than that in the wild type (lines labeled T). (**J**) Fluorescent micrograph showing a larva with almost complete rounded-up muscles as revealed by staining for Mhc. (**K**) Fura PE 3 ratiometric calcium imaging micrographs of primary muscles derived from embryos of wild type (top) and *UAS-Dcr-2/+; Dmef2-Gal4/UAS-CG2165 hp* (bottom) and cultured at 25°C for 3 days. The color indicates the ratio between the emission intensities excited at 340 nm and 380 nm, and reflects a measurement of calcium concentration. (**L**) Bar chart showing $[Ca^{2+}]_i$ as average±s.e.m. for wild-type control cells (0.344±0.0162 μM; *n*=35 muscle cells in two representative experiments, white bar), and for muscle-specific CG2165 RNAi (0.0105±0.0012 μM; *n*=71 in three representative experiments, gray bar). Scale bars: 50 μm in A for A-E; 20 μm in H for H,I; 75 μm in J.

compared with control larvae of the same age (Fig. 6G). These phenotypes indicated that muscle contraction was not affected because defects in contraction would have been expected to lead to an elongated body. We further examined the muscle morphology of muscle-specific *CG2165* RNAi larvae by fluorescent confocal microscopy (Fig. 6H-J). The stainings for Mhc and Actn revealed that some larvae showed almost completely rounded-up muscles (Fig. 6J), whereas others still contained muscles with recognizable striated morphology (Fig. 6I). This is in contrast to control larvae of the same age, which always had nicely patterned muscles (Fig. 6H). Moreover, those muscles that still had the striated myofibril structure also exhibited a hypercontracted morphology, as indicated by their dramatically shortened sarcomere sizes and muscle lengths (Fig. 6I). We further investigated whether disruption of *CG2165* would lead to increased $[Ca^{2+}]_i$ in muscles. We conducted single-cell calcium imaging using Fura PE 3 on primary muscle cells derived from muscle-specific *CG2165* RNAi embryos (Fig. 6K,L) and found that the $[Ca^{2+}]_i$ in these primary muscles was over 30 times higher than that in wild-type control muscles (Fig. 6L). This confirmed that the phenotypes observed in the muscle-specific *CG2165* RNAi larvae were associated with an abnormal increase in $[Ca^{2+}]_i$ in muscle cells. Altogether, our findings suggest that *Drosophila* PMCA plays an important role in maintaining muscle integrity.

DISCUSSION

Drosophila primary cultures have been used to study muscle biology in normal and mutant animals (Donady and Seecof, 1972; Volk et al., 1990). A significant advantage of this approach is that it obviates the difficulty associated with the dissection of early first instar larvae and allows visualization of myofibril organization at a cellular level using conventional microscopy. Here, we have established a robust method for RNAi screening in *Drosophila* primary cells and found that simple bathing of these cells in dsRNA-containing medium is sufficient for an effective and specific RNAi effect. This technology allows the analysis of late-stage differentiation processes such as muscle assembly and maturation, which is difficult to tackle with classical *Drosophila* genetics.

Drosophila primary cultures have distinct advantages over vertebrate culture systems for systematically analyzing gene functions involved in muscle assembly and maintenance. Myotube cultures derived from primary myoblasts in vertebrates can have a high degree of sarcomeric maturity, and thus are often used for studies on myofibril assembly. However, preparations of primary myoblasts from freshly harvested tissues can be technically demanding, time consuming and costly (Cooper et al., 2004), in contrast to the ease with which large numbers of *Drosophila* primary cells can be isolated from embryos. Established vertebrate clonal muscle cell lines such as C2C12 have overcome the requirement for repeated myoblast isolation from fresh tissue (Cooper et al., 2004). Despite extensive fusion and myotube formation during early stages of differentiation, it has been difficult to derive C2C12 myotubes with a mature sarcomeric structure using traditional culture methods, although co-culturing cells on a primary fibroblast substratum has been reported to be more successful (Cooper et al., 2004). *Drosophila* primary cultures, however, consist of mixed cell populations, whereby non-muscle cells may facilitate muscle differentiation (J.B., unpublished). The method described in this study, however, might not be very useful for identifying genes involved in myoblast fusion, as newly isolated myoblasts have already adopted their cell-intrinsic developmental programs and have expressed those proteins required for fusion (Fig. 1) (Estrada et al., 2006). In addition, fusion takes place 2 hours after plating at 25°C and 7 hours at 18°C, too short a time to allow efficient RNAi (J.B., J. Lu, A. Michelson and N.P., unpublished).

In this study, we have described four distinct muscle phenotypes associated with knock-down of *Drosophila* homologs of human genes involved in muscle diseases. Both congenital myopathies and cardiomyopathies are also called 'sarcomere diseases' (Bornemann and Goebel, 2001; Clarkson et al., 2004; Seidman and Seidman, 2001). Indeed, the primary muscle phenotypes caused by RNAi on the *Drosophila* homologs of these human disease genes indicate that they are involved in different aspects of sarcomeric organization and muscle maintenance. Furthermore, we used this approach to conduct a screen to identify genes involved in muscle assembly and maintenance. In addition to the genes already discussed, we found that several of the proteins encoded by Class II genes are components of various cellular machineries. For example, four proteins are related to the ubiquitin/proteosome system (UPS), whereas four others function in metabolic pathways, and five are involved in basic transcription or translation. This indicates that development and maintenance of striated muscles rely on the turnover of regulatory and structural components as well as the maintenance of metabolic homeostasis in muscles (Hass et al., 2007; Lecker et al., 2006). In addition, three genes encoding ribosomal protein components were identified as Class IV genes that regulate muscle myofibril size. Of note, 22 genes identified from the screen have not been previously reported to be involved in late muscle differentiation (see Table S2 in the supplementary material).

Furthermore, we have demonstrated that the in vivo functions in muscle of genes identified from this approach can be validated and further characterized by injecting dsRNAs into embryos (Kennerdell and Carthew, 1998), by expressing snap-back hairpin constructs (Dietzl et al., 2007; Ni et al., 2008), or by using genetic mutations that disrupt gene function (Bai et al., 2007). Here, we have confirmed in vivo the primary muscle RNAi phenotypes of *Fit1*, *Fit2* and *CG2165*. In particular, we have analyzed the effects of *CG2165*, a previously uncharacterized gene identified from this screen, on the maintenance of muscle cell integrity in primary cell culture as well as in vivo. Our results demonstrate that disruption of *Drosophila* PMCA does not affect muscle development or contraction, but rather the excitation-contraction coupling process. Importantly, single-cell calcium imaging in primary muscles derived from muscle-specific *CG2165* RNAi embryos reveals that the increased $[Ca^{2+}]_i$ could be the primary cause of the rounded-up muscle phenotypes. Although we expect that the majority of the genes identified from this screen act autonomously in muscles, some genes expressed in tendons or neurons, such as *mew* (Estrada et al., 2007) and *Mgat2* (Tsitilou and Grammenoudi, 2003), may affect muscle morphology in a non-cell-autonomous manner. Further in vivo verification will be needed to address the tissue specificity of these genes by knocking down their function in a tissue-specific manner.

Our demonstration that RNAi works effectively in primary cells broadens considerably the types of studies that can be undertaken with *Drosophila* primary cultures. The major advantage of using primary cells for functional genomics is that they better model their in vivo counterparts than do immortalized mammalian cells. As the different cell types can be tracked in primary cultures using a tissue-specific GFP, antibodies or other markers, primary-cell-based RNAi screens may be used to identify genes required in other differentiated cells as well [e.g. primary neurons (K. Sepp and N.P., unpublished) (Sharma and Nirenberg, 2007)]. Importantly, RNAi screens in *Drosophila* primary cultures can be carried out by a simple bathing

method for dsRNA uptake. This is in contrast to the difficulties that have been reported with RNAi in mammalian cell lines and primary cells, which requires delivery of siRNAs into cells by chemical transfection or electroporation (Ovcharenko et al., 2005; Sharma and Nirenberg, 2007).

We anticipate that RNAi in primary cells will contribute to the understanding of human muscle biology in a number of ways. First, further deciphering the molecular relationships among genes whose RNAi phenotypes belong to the same phenotypic class will help frame the molecular mechanisms underlying muscle assembly, both in normal development and in pathological conditions. This approach might reveal candidate molecules for myopathies whose genetic lesions have not yet been identified. Second, using the Gal4/UAS system (Brand and Perrimon, 1993), expression of wild-type or mutant proteins relevant to human diseases in primary cells will lead to the development of cell-based assays to model human diseases that can then be used for RNAi and small-molecule screens. For example, RNAi in primary cells from *Drosophila* embryos overexpressing Actins with dominant mutations that cause human nemaline myopathy can be used to dissect the molecular mechanisms underlying the formation of nemaline rods under pathological conditions. Our study provides a paradigm for the use of *Drosophila* primary cells in designing cell-based assays for functional genomics using such screens.

We thank Drs W. Chia, E. Olson, A. Michelson, J. Saide, H. Nguyen, A. Paulula, and G. Lnenicka and the *Drosophila* Bloomington Stock Center for fly stocks and antibodies; D. Devenport and N. Brown for sharing their unpublished data on *Fit1* and *Fit2*; J. Lu and A. Michelson for an initial collaboration on applying RNAi to primary cultured cells; K. Sepp for collaboration on large-scale primary culture techniques; the members of the *Drosophila* RNAi Screening Center for technical support; and B. Mathey-Prevot for critical comments on the manuscript. This work was partially supported by the Damon Runyon Cancer Research Foundation Fellowship DRG-1716-02 to J.B. and a NIH grant R01-AG02250 to H.-S.L. N.P. is an Investigator of the Howard Hughes Medical Institute.

Supplementary material

Supplementary material for this article is available at http://dev.biologists.org/cgi/content/full/135/8/1439/DC1

References

Arbrecht, S., Wang, S., Holz, A., Bergter, A. and Paululat, A. (2006). The ADAM metalloprotease Kuzbanian is crucial for proper heart formation in *Drosophila melanogaster*. *Mech. Dev.* **123**, 327-387.

Bai, J., Hartwig, J. H. and Perrimon, N. (2007). SALS, a WH2-domain-containing protein, promotes sarcomeric actin filament elongation from pointed ends during *Drosophila* muscle growth. *Dev. Cell* **13**, 828-842.

Bate, M. (1990). The embryonic development of larval muscles in *Drosophila*. *Development* **110**, 791-804.

Bate, M. (1993). The mesoderm and its derivatives. In *The Development of Drosophila melanogaster*. Vol. 2 (ed. M. Bate and A. Martinez-Arias), pp. 1013-1090. New York: Cold Spring Harbor Laboratory Press.

Baylies, M., Bate, M. and Gomez, M. R. (1998). Myogenesis: a view from *Drosophila*. *Cell* **93**, 921-927.

Bernstein, S., Fyrberg, E. and Donady, J. (1978). Isolation and partial characterization of *Drosophila* myoblasts from primary cultures of embryonic cells. *J. Cell Biol.* **78**, 856-865.

Bernstein, S., O'Donnell, P. and Cripps, R. (1993). Molecular genetic analysis of muscle development, structure, and function in *Drosophila*. *Int. Rev. Cytol.* **143**, 63-152.

Bornemann, A. and Goebel, H. (2001). Congenital myopathies. *Brain Pathol.* **11**, 206-217.

Bour, B., O'Brien, M., Lockwood, W., Goldstein, E., Bodmer, R., Taghert, P., Abmayr, S. and Nguyen, H. (1995). *Drosophila* MEF2, a transcription factor that is essential for myogenesis. *Genes Dev.* **9**, 730-741.

Brand, A. and Perrimon, N. (1993). Targeted gene expression as a means of altering cell fates and generating dominant phenotypes. *Development* **118**, 401-415.

Chen, E. and Olson, E. (2001). Antisocial, an intracellular adaptor protein, is required for myoblast fusion in *Drosophila*. *Dev. Cell* **1**, 705-715.

Chen, E. and Olson, E. (2004). Towards a molecular pathway for myoblast fusion in *Drosophila*. *Trends Cell Biol.* **14**, 452-460.

Chien, S., Reiter, L., Bier, E. and Gribskov, M. (2002). Homophila: human disease gene cognates in *Drosophila*. *Nucleic Acids Res.* **30**, 149-151.

Clark, K., McElhinny, A., Beckerle, M. and Gregorio, C. (2002). Striated muscle cytoarchitecture: an intricate web of form and function. *Annu. Rev. Cell Dev. Biol.* **18**, 637-706.

Clarkson, E., Costa, C. and Macheskv, L. (2004). Congenital myopathies: diseases of the actin cytoskeleton. *J. Pathol.* **204**, 407-417.

Clemens, J., Worby, C., Simonson-Leff, N., Muda, M., Maehama, T., Hemmings, B. and Dixon, J. (2000). Use of double-stranded RNA interference in *Drosophila* cell lines to dissect signal transduction pathways. *Proc. Natl. Acad. Sci. USA* **97**, 6499-6503.

Cooper, S., Maxwell, A., Kizana, E., Ghoddusi, M., Hardeman, E., Alexander, I., Allen, D. and North, K. (2004). C2C12 co-culture on a fibroblast substratum enables sustained survival of contractile, highly differentiated myotubes with peripheral nuclei and adult fast myosin expression. *Cell Motil. Cytoskeleton* **58**, 200-211.

Cox, R. T. and Spradling, A. C. (2003). A Balbiani body and the fusome mediate mitochondrial inheritance during *Drosophila* oogenesis. *Development* **130**, 1579-1590.

Dalkilic, I. and Kunkel, L. M. (2003). Muscular dystrophies: genes to pathogenesis. *Curr. Opin. Genet. Dev.* **13**, 231-238.

Dietzl, G., Chen, D., Schnorrer, F., Su, K., Barinova, Y., Fellner, M., Gasser, B., Kinsey, K., Oppel, S., Scheiblauer, S. et al. (2007). A genome-wide transgenic RNAi library for conditional gene inactivation in *Drosophila*. *Nature* **448**, 151-156.

Donady, J. and Seecof, R. (1972). Effect of the gene *lethal (1) myospheroid* on *Drosophila* embryonic cells in vitro. *In Vitro* **8**, 7-12.

Duan, H., Skeath, J. and Nguyen, H. (2001). *Drosophila* Lame duck, a novel member of the Gli superfamily, acts as a key regulator of myogenesis by controlling fusion-competent myoblast development. *Development* **128**, 4489-4500.

Echalier, G. (1997). Primary cell cultures of *Drosophila* cells. In *Drosophila Cells in Culture* (ed. G. Echalier), pp. 71-127. London: Academic Press.

Estrada, B., Choe, S., Gisselbrecht, S., Michaud, S., Raj, L., Busser, B., Halfon, M., Church, G. and Michelson, A. (2006). An integrated strategy for analyzing the unique developmental programs of different myoblast subtypes. *PLoS Genet.* **2**, e16.

Estrada, B., Gisselbrecht, S. and Michelson, A. (2007). The transmembrane protein Perdido interacts with Grip and integrins to mediate myotube projection and attachment in the *Drosophila* embryo. *Development* **134**, 4469-4478.

Grynkiewicz, G., Poenie, M. and Tsien, R. (1985). A new generation of Ca2+ indicators with greatly improved fluorescence properties. *J. Biol. Chem.* **260**, 3440-3450.

Gustafson, K. and Boulianne, G. (1996). Distinct expression patterns detected within individual tissues by the Gal4 enhancer trap technique. *Genome* **39**, 174-182.

Gwack, Y., Sharma, S., Nardone, J., Tanasa, B., Iuga, A., Srikanth, S., Okamura, H., Bolton, D., Feske, S., Hogan, P. et al. (2006). A genome-wide *Drosophila* RNAi screen identifies DYRK-family kinases as regulators of NFAT. *Nature* **441**, 646-650.

Halfon, M., Gisselbrecht, S., Lu, J., Estrada, B., Keshishian, H. and Michelson, A. (2002). New fluorescent protein reporters for use with the *Drosophila* Gal4 expression system and for vital detection of balancer chromosomes. *Genesis* **34**, 135-138.

Hass, K., Woodruff, E. and Broadie, K. (2007). Proteasome function is required to maintain muscle cellular architecture. *Biol. Cell* **99**, 615-626.

Hauptmann, G. and Gerster, T. (2000). Multicolor whole-mount in situ hybridization. *Methods Mol. Biol.* **137**, 139-148.

Kennerdell, J. and Carthew, R. (1998). Use of dsRNA-mediated genetic interference to demonstrate that *frizzled* and *frizzled 2* act in the wingless pathway. *Cell* **95**, 1017-1026.

Kermode, J. C., Zheng, Q. and Milner, E. P. (1990). Marked temperature dependence of the platelet calcium signal induced by human von Willebrand factor *Blood* **94**, 199-207.

Kulkarni, M., Booker, M., Silver, S., Friedman, A., Hong, P., Perrimon, N. and Mathey-Prevot, B. (2006). Evidence of off-target effects associated with long dsRNAs in *Drosophila melanogaster* cell-based assays. *Nat. Methods* **3**, 833-838.

Lecker, S., Goldberg, A. and Mitch, W. (2006). Protein degradation by the ubiquitin-proteasome pathway in normal and disease states. *J. Am. Soc. Nephrol.* **17**, 1807-1819.

Lnenicka, G. A., Grizzaffi, J., Lee, B. and Rumpal, N. (2006). Ca2+ dynamics along identified synaptic terminals in *Drosophila* larvae. *J. Neurosci.* **26**, 12283-12293.

Ma, Y., Creanga, A., Lum, L. and Beachy, P. (2006). Prevalence of off-target effects in *Drosophila* RNA interference screens. *Nature* **443**, 359-363.

MacKrell, A., Blumberq, B., Haynes, S. and Fessler, J. (1988). The lethal *myospheroid* gene of *Drosophila* encodes a membrane protein homologous to vertebrate integrin beta subunits. *Proc. Natl. Acad. Sci. USA* **85**, 2633-2637.

Mandal, L., Dumstrei, K. and Hartenstein, V. (2004). Role of FGFR signaling in the morphogenesis of the *Drosophila* visceral musculature. *Dev. Dyn.* **231**, 342-348.
Morin, X., Daneman, R., Zavortink, M. and Chia, W. (2001). A protein trap strategy to detect GFP-tagged proteins expressed from their endogenous loci in *Drosophila*. *Proc. Natl. Acad. Sci. USA* **98**, 15050-15055.
Ni, J.-Q., Markstain, M., Binari, R., Pfeiffer, B., Liu, L.-P., Villalta, C., Booker, M., Perkins, L. and Perrimon, N. (2008). Vector and parameters for targeted transgenic RNA interference in *Drosophila melanogaster*. *Nat. Methods* **5**, 49-51.
Nongthomba, U., Clark, S., Cummins, M., Ansari, M., Stark, M. and Sparrow, J. C. (2004). Troponin I is required for myofibrillogenesis and sarcomere formation in *Drosophila* flight muscle. *J. Cell Sci.* **117**, 1795-1805.
O'Donnell, P. and Bernstein, S. (1988). Molecular and ultrastructural defects in a *Drosophila myosin heavy chain* mutant: differential effects on muscle function produced by similar thick filament abnormalities. *J. Cell Biol.* **107**, 2601-2612.
Ovcharenko, D., Jarvis, R., Hunicke-Smith, S., Kelnar, K. and Brown, D. (2005). High-throughput RNAi screening in vitro: from cell lines to primary cells. *RNA* **11**, 985-993.
Ranganavakulu, G., Schulz, R. and Olson, E. (1996). Wingless signaling induces nautilus expression in the ventral mesoderm of the *Drosophila* embryo. *Dev. Biol.* **176**, 143-148.
Rogalski, T., Mullen, G., Gilbert, M., Williams, B. and Moerman, D. (2000). The UNC-112 gene in *Caenorhabditis elegans* encodes a novel component of cell-matrix adhesion structures required for integrin localization in the muscle cell membrane. *J. Cell Biol.* **150**, 253-264.
Roos, J., DiGregorio, P., Yeromin, A., Ohlsen, K., Lioudyno, M., Zhang, S., Safrina, O., Kozak, J., Wagner, S., Cahalan, M. et al. (2005). STIM1, an essential and conserved component of store-operated Ca2+ channel function. *J. Cell Biol.* **169**, 435-445.
Ruiz-Gomez, M., Coutts, N., Price, A., Taylor, M. and Bate, M. (2000). *Drosophila* dumbfounded: a myoblast attractant essential for fusion. *Cell* **102**, 189-198.
Sandmann, T., Jensen, L. J., Jakobsen, J. S., Karzynski, M. M., Eichenlaub, M. P., Bork, P. and Furlong, E. E. (2006). A temporal map of transcription factor activity: mef2 directly regulates target genes at all stages of muscle development. *Dev. Cell* **10**, 797-807.
Seidman, J. and Seidman, C. (2001). The genetic basis for cardiomyopathy: from mutation identification to mechanistic paradigms. *Cell* **104**, 557-567.
Sharma, S. and Nirenberg, M. (2007). Silencing of genes in cultured *Drosophila* neurons by RNA interference. *Proc. Natl. Acad. Sci. USA* **104**, 12925-12930.
Storti, R., Horovitch, S., Scott, M., Rich, A. and Pardue, M. (1978). Myogenesis in primary cell cultures from *Drosophila melanogaster*: protein synthesis and actin heterogeneity during development. *Cell* **13**, 589-598.
Tsitilou, S. and Grammenoudi, S. (2003). Evidence for alternative splicing and developmental regulation of the *Drosophila melanogaster Mgat2* (N-acetylglucosaminyltransferase II) gene. *Biochem. Biophys. Res. Commun.* **312**, 1372-1376.
Tucker, J. B., Backie, J. B., Cottam, D. M., Rogers-Bald, M. M., Macintyre, J., Scarborough, J. A. and Milner, M. J. (2004). Positioning and capture of cell surface-associated microtubules in epithelial tendon cells that differentiate in primary embryonic *Drosophila* cell cultures. *Cell Motil. Cytoskeleton* **57**, 175-185.
Vigoreaux, J. O. (2001). Genetics of the *Drosophila* flight muscle myofibril: a window into the biology of complex systems. *BioEssays* **23**, 1047-1063.
Volk, T., Fessler, L. and Fessler, J. (1990). A role for integrin in the formation of sarcomeric cytoarchitecture. *Cell* **63**, 525-536.
Zhang, Y., Featherstone, D., Davis, W., Rushton, E. and Broadie, K. (2000). *Drosophila D-titin* is required for myoblast fusion and skeletal muscle striation. *J. Cell Sci.* **113**, 3103-3115.

Table S1. Muscle disease genes, their *Drosophila* homologs and their primary RNAi muscle phenotypes

Disease genes	Gene product	E-value	Fly homolog	Fbgn#	RNAi phenotypes
Congenital myopathies					
NEB	Nebulin	6.30E-12	Lasp	FBgn0063485	Class I
ACTA1	Alpha-actin, skeletal	0	Act57B	FBgn0000044	Class IV
		0	Act42A	FBgn0000043	Class IV
		0	Act87E	FBgn0000046	Class IV
		0	Act5C	FBgn0000042	Class IV
TPM1; TPM2	Alpha, beta-tropomyosin	7.60E-45	Tm1	FBgn0003721	N
TNNT1	Slow troponin T	6.30E-06	up	FBgn0004169	Class III
MTM1	Myotubularin	0	mtm	FBgn0025742	Class II
RYR1	Ryanodin receptor	0	Rya-r44F	FBgn0011286	Class III
ITGA7	Integrin alpha7	6.00E-88	mew	FBgn0004456	Class I
Cardiomyopathies					
FHC1 (MYH6, MYH7)	Cardiac myosin heavy chain	0	Mhc	FBgn0002741	Class III
FHC2 (=TTNT2)	Cardiac troponin T		up	FBgn0004169	Class III
FHC3 (MyBP-C)	Cardiac myosin binding protein-C	1.30E-69	sls	FBgn0003432	Class II
MYL2	Regulatory myosin light chain	2.00E-41	sqh	FBgn0003514	Class II
		8.00E-27	mlc2	FBgn0002773	Class III
MYL3	Essential myosin light chain	4.00E-34	mlc-c	FBgn0004687	N
TNNI3 (=TNNCI)	Cardiac troponin I	3.00E-06	wupA	FBgn0004028	Class III
FHC9	Titin: myosin light chain kinase	0	bt		Class III
CMD1G (=TTN)	Titin	0	bt	FBgn0005666	Class III
VCL	Vinculin	1.00E-92	Vinc	FBgn0004397	Class IV
ARVD2 (=RYR2)	Ryanodin receptor	0	Rya-r44F	FBgn0011286	Class III
G4.5	Tafazzin	2.00E-58	tafazzin	FBgn0026619	Class II
Muscular dystrophies					
DMD	Dystrophin	0	Dys	FBgn0024242	N
LMNA	LaminA/C	4.90E-79	Lam	FBgn0002525	N
DYSF	Dysferlin	2.20E-93	mfr	FBgn0035935	N
SGCG	Sarcoglycan, gamma	1.00E-43	Scgdelta	FBgn0025391	N
CAPN3	Calpain-3	1.00E-178	CalpB	FBgn0025866	Class III
SGCA	Sarcoglycan, alpha	3.00E-13	Scgalpha	FBgn0032013	N
SGCD	Sarcoglycan, delta	6.00E-48	Scgdelta	FBgn0025391	N
TRIM32	TRIM32	7.00E-15	CG15105	FBgn0034412	Class II
LAMA2	Laminin alpha 2	0	wb	FBgn0004002	N

Human muscle disease genes were selected based on the gene lists from Bornemann and Goebel (Bornemann and Goebel, 2001), Clarkson et al. (Clarkson et al., 2004) for congenital myopathies; Seidman and Seidman (Seidman and Seidman, 2001) for cardiomyopathies; the MDA website (http://www.mdausa.org/disease/) and Dalkilic and Kunkel (Dalkilic and Kunkel, 2003) for muscular dystrophies. *Drosophila* genes that are homologous to human disease genes were chosen based on their protein homology with the lowest E value (and at least ⩽–5) for a match to human protein (BLASTP) in Homophila (http://superfly.ucsd.edu/homophila/) (Chien et al., 2002), as well as their expression in muscle tissues (http://www.fruitfly.org/cgi-bin/ex/insitu.pl). Information on the dsRNAs targeting the *Drosophila* genes is available in Table S2 and from http://flyrnai.org/. The various phenotypic classes are indicated (see text).
N, no muscle phenotypes.

Table S2. List of hits identified from the RNAi screen as potential regulators of muscle assembly

						Expression in myoblasts and/or muscles		
							Microarray data (increased expression)	
Comments	Gene name	FBgn#	Human homolog	Protein domains	Molecular function	BDGP in situ	Furlong lab.	Michelson lab.
Class I. Muscles are rounded up								
Severe	CG2165	FBgn0025704	ATP2B3	Calcium-translocating P-type ATPase, PMCA-type	Calcium-transporting ATPase activity	N/A	Yes	No
Medium	Fit1	FBgn0035498	PLEKHC1	FERM, Pleckstrin-like, Band 4.1, PH	Cell adhesion molecule binding	N/A	Yes	N/A
Medium	Idh	FBgn0001248	IDH1	Isocitrate dehydrogenase NADP-dependent	Isocitrate dehydrogenase ($NADP^+$) activity	N/A	No	No
Medium	Fit2	FBgn0036688	PLEKHC1	FERM, Pleckstrin homology-type, Band 4.1	Cell adhesion molecule binding	N/A	Yes	No
Class II. Muscles are spread, myosin filaments still show a striated pattern, but actin filaments show no discernible striations								
Severe	CG6640	FBgn0036068		Sugar transporter superfamily	Transporter activity	N/A	No	No
Severe	eIF-4E	FBgn0015218	EIF4E	Eukaryotic translation initiation factor 4E (eIF-4E)	Translation	N/A	No	N/A
Severe	Pros26	FBgn0002284	PSMB1	20S proteasome, A and B subunits	Endopeptidase activity	Yes	Yes	N/A
Severe	CG8789	FBgn0036896	MAP3K12	Protein kinase	Protein kinase activity	N/A	No	N/A
Severe	Prosbeta2	FBgn0023174	PSMB7	20S proteasome, A and B subunits,	Mitosis and meiosis	N/A	Yes	Yes
Severe	abs	FBgn0015331	DDX41	DEAD/DEAH box helicase	ATP-dependent RNA helicase activity	N/A	Yes	No
Severe	CG9779	FBgn0037231	VPS24	Snf7	Vacuolar protein sorting 24	N/A	No	N/A
Severe	CG9776	FBgn0027866		Zn-finger, C2H2 type	Nucleic acid binding, zinc ion binding	N/A	N/A	N/A
Severe	Taf4	FBgn0010280	TAF4B	Transcription initiation factor TFIID component TAF	Transcription initiation factor activity	Yes	No	No
Severe	CG14648	FBgn0037245		5-formyltetrahydrofolate cyclo-ligase	Catalytic activity	N/A	N/A	No
Severe	CG5027	FBgn0036579		Thioredoxin domain 2, Thioredoxin-related, Calsequestrin	Electron transporter activity	No	N/A	N/A
Severe	CG31523	FBgn0051523		Multicopper oxidase, copper-binding site	Acyltransferase activity; copper ion binding	Yes	Yes	No
Severe	pygo	FBgn0043900	PYGO2	Zn-finger-like, PHD finger, Aminoacyl-tRNA synthetase	DNA binding; ATP binding; tRNA ligase activity; protein binding	N/A	Yes	No
Severe	deltaCOP	FBgn0028969	ARCN1	Longin-like, Mu2 adaptin subunit (AP50) of AP2		N/A	No	No
Severe	CG1890	FBgn0039869	TBCA	Tubulin binding cofactor A	Unfolded protein binding	N/A	Yes	No
Severe	CG3457	FBgn0024984		N/A	N/A	N/A	N/A	N/A
Severe	PH4alphaNE1	FBgn0039780		Tetratricopeptide-like helical, Hpt, Prolyl 4-hydroxylase,	Procollagen-proline 4-dioxygenase activity	N/A	N/A	N/A
Severe	lva	FBgn0029688		Microfilament/microtubule-associated proteins (MMAPs)	Actin binding; microtubule binding; protein binding; spectrin binding	N/A	N/A	N/A

Medium	CG6020	FBgn0037001	NDUFA9	N/A	NADH dehydrogenase (ubiquinone) activity	Yes	N/A	N/A
Medium	CG6014	FBgn0027542		N/A	N/A	N/A	N/A	N/A
Medium	atms	FBgn0010750	PD2	RNA polymerase II associated, Paf1	Kinesin activity	N/A	N/A	N/A
Medium	CG1544	FBgn0039827	DHTKD1	Transketolase, central region, 2-oxoglutarate dyhydrogenase E1 component		N/A	Yes	No
Medium	Nf1	FBgn0015269	NF1	Rho GTPase activation protein, Ras GTPase-activating protein, Cellular retinaldehyde-binding)/triple function, C-, HEAT	Ras GTPase activator activity; receptor binding	N/A	Yes	N/A
Medium	Mgat2	FBgn0039738	MGAT2	N-acetylglucosaminyltransferase II		No	Yes	No
Severe	RhoGAP100F	FBgn0039883		PDZ/DHR/GLGF, RhoGAP, C2	GTPase activator activity; receptor binding	N/A	Yes	No
Severe	Actn	FBgn0000667	ACTN1	EF-Hand type, Actin-binding, actinin-type	Actin filament binding	N/A	Yes	No
Severe	Rpn1	FBgn0028695	PSMD2	Proteasome/cyclosome, regulatory subunit	Endopeptidase activity,enzyme regulatory activity	N/A	No	N/A
Severe	Rpn2	FBgn0028692	PSMD1	Proteasome/cyclosome, regulatory subunit	Endopeptidase activity,enzyme regulatory activity	N/A	Yes	No
Class III. Muscles are spread, and both actin and myosin filaments lack striation								
Severe	Prm	FBgn0003149		Myosin tail	Striated muscle thick filament	N/A	Yes	No
Severe	bt	FBgn0005666		Protein kinase-like, Fibronectin, type III-like fold	Myosin-light-Chain kinase activity	N/A	Yes	No
Severe	Mlc2	FBgn0002773	MYL2	EF-Hand type, Calcium-binding EF-hand	Microfilament motor activity	N/A	Yes	No
Severe	Tmod	FBgn0082582	TMOD1	Tropomodulin	Tropomyosin binding; actin binding;	N/A	Yes	No
Medium	polo	FBgn0003124	PLK1	POLO box duplicated region, Protein kinase	Receptor signaling protein serine/threonine kinase activity	N/A	Yes	Yes
Class IV. Muscles with short and/or thin myofibrils								
Severe	Ac76E	FBgn0004852		Guanylate cyclase	Guanylate cyclase activity, G protein coupled receptor pathway	N/A	Yes	No
Severe	CG5931	FBgn0036548	ASCC3L1	DEAD/DEAH box helicase, Sec63	ATP-dependent RNA helicase activity	N/A	Yes	No
Severe	CG31374	FBgn0051374		Actin binding WH2 domains	Actin binding, actin assembly	N/A	No	No
Severe	CG8636	FBgn0029629	EIF3S4	Zn-finger, CCHC type, RNA-binding region RNP-1	Translation initiation factor activity;	Yes	No	No
Severe	CG8743	FBgn0036904	MCOLN3	Cation (not K+) channel, Ca2+/Na+ channel	Calcium channel activity	N/A	No	No
Severe	crn	FBgn0000377	CRNKL1	Phosphatidylinositol transfer protein-like, N-termi	Pre-mRNA splicing factor activity; transporter activity	N/A	No	No
Severe	Taf2	FBgn0011836	TAF2	N-6 Adenine-specific DNA methylase	General RNA polymerase transcription factor activity	Yes	No	No
Severe	Trn	FBgn0024921	TNPO1	Armadillo-like helical, Importin-beta, N-terminal,	Protein carrier activity	N/A	N/A	No

Severe	Vinc	FBgn0004397	VCL	Vinculin/alpha-catenin, Vinculin	Actin binding; structural constituent of cytoskeleton	N/A	N/A	No
Severe	RpL4	FBgn0003279	RPL4	Ribosomal protein L4/L1e	Nucleic acid binding;structural constituent of ribosome	N/A	No	No
Severe	RpS12	FBgn0014027	RPS12	Ribosomal protein L7Ae/L30e/S12e/Gadd45	Nucleic acid binding;structural constituent of ribosome	Yes	No	No
Severe	RpS9	FBgn0010408	RPS9	RNA-binding S4, Ribosomal protein S4/9,	Nucleic acid binding;structural constituent of ribosome	N/A	Yes	No

RNAi phenotypes could be observed with an independent second set of amplicons. The hits are grouped into four distinct phenotypic classes (see Results) and are listed by the severity of their RNAi muscle phenotypes in primary culture. Human orthologs were determined by reciprocal BLASTP. The putative expression of *Drosophila* genes in the mesoderm (either myoblasts and/or muscles) were based on the Berkeley *Drosophila* Genome Project (BDGP) in situ expression database (http://www.fruitfly.org/cgi-bin/ex/insitu.pl), Dmef2 loss-of-function microarray database [the fold enrichment log2 (mutant/wild type) is at least 0.5 or lower] (Sandmann et al., 2006) and Dmef2 chip-on-chip database (Sandmann et al., 2006) (http://furlonglab.embl.de/data), and myoblast gene expression database [the fold enrichment log2 (mutant/wild type) is at least 0.7 or lower] (Estrada et al., 2006).

Table S3. List of amplicons for generating dsRNAs targeting the genes that are listed in Table S2

Gene name	FBgn#	Amplicons
CG2165	FBgn0025704	DRSC17113, DRSC17114, DRSC17154, DRSC34373
Fit1	FBgn0035498	DRSC08450, DRSC34432
Idh	FBgn0001248	DRSC10779, DRSC34441
Fit2	FBgn0036688	DRSC10908, DRSC32125
CG6640	FBgn0036068	DRSC10681, DRSC34404
eIF-4E	FBgn0015218	DRSC11342, DRSC32113
Pros26	FBgn0002284	DRSC11256, DRSC32168
CG8789	FBgn0036896	DRSC11046, DRSC34410
Prosbeta2	FBgn0023174	DRSC11257, DRSC32178
abs	FBgn0015331	DRSC12372, DRSC31883
CG9779	FBgn0037231	DRSC12332, DRSC34417
CG9776	FBgn0027866	DRSC12127, DRSC34415
Taf4	FBgn0010280	DRSC11297, DRSC31762
CG14648	FBgn0037245	DRSC12002, DRSC34034
CG5027	FBgn0036579	DRSC10471, DRSC34391
CG31523	FBgn0051523	DRSC12009, DRSC34377, DRSC34378
pygo	FBgn0043900	DRSC14322, DRSC33088
deltaCOP	FBgn0028969	DRSC18760, DRSC31062, DRSC31063
CG1890	FBgn0039869	DRSC15395, DRSC29064
CG3457	FBgn0024984	DRSC18509, DRSC34386
PH4alphaNE1	FBgn0039780	DRSC16546, DRSC34461, DRSC34462
lva	FBgn0029688	DRSC18403, DRSC31278, DRSC31279
CG6020	FBgn0037001	DRSC11791, DRSC34398, DRSC34399
CG6014	FBgn0027542	DRSC11609, DRSC34396, DRSC34397
atms	FBgn0010750	DRSC12310, DRSC34353, DRSC34354
CG1544	FBgn0039827	DRSC15036, DRSC34369, DRSC34370
Nf1	FBgn0015269	DRSC16758, DRSC34456, DRSC34457
Mgat2	FBgn0039738	DRSC16347, DRSC34446, DRSC34447
RhoGAP100F	FBgn0039883	DRSC15409, DRSC34466, DRSC34467
Actn	FBgn0000667	DRSC17724, DRSC34351, DRSC34352
Rpn1	FBgn0028695	DRSC11274, DRSC32192, DRSC32193
Rpn2	FBgn0028692	DRSC16839, DRSC32198, DRSC32199
Prm	FBgn0003149	DRSC11255, DRSC36327, DRSC36328
bt	FBgn0005666	DRSC17129, DRSC17171, DRSC34355, DRSC34356
Mlc2	FBgn0002773	DRSC16741, DRSC32500, DRSC32501
Tmod	FBgn0082582	DRSC17062, DRSC34480, DRSC34481
polo	FBgn0003124	DRSC11384, DRSC34463, DRSC34464
Ac76E	FBgn0004852	DRSC09642, DRSC32652, DRSC32653
CG5931	FBgn0036548	DRSC10559, DRSC32419, DRSC32420
CG31374	FBgn0051374	DRSC14925, DRSC16113, DRSC32900, DRSC32901
CG8636	FBgn0029629	DRSC18427, DRSC32088
CG8743	FBgn0036904	DRSC11032, DRSC31589, DRSC31590
crn	FBgn0000377	DRSC18184, DRSC31852, DRSC31853
Taf2	FBgn0011836	DRSC11298, DRSC33206, DRSC33207
Trn	FBgn0024921	DRSC11309, DRSC32777, DRSC32778
Vinc	FBgn0004397	DRSC18728, DRSC31286, DRSC31287
RpL4	FBgn0003279	DRSC16833, DRSC32560, DRSC32561
RpS12	FBgn0014027	DRSC11270, DRSC34294
RpS9	FBgn0010408	DRSC11273, DRSC32598, DRSC32599
Lasp	FBgn0063485	DRSC10379, DRSC34926, DRSC34927
Act57B	FBgn0000044	DRSC04042, DRSC31414
Act42A	FBgn0000043	DRSC04835, DRSC25061
Act87E	FBgn0000046	DRSC22578, DRSC23961
Act5C	FBgn0000042	DRSC17723, DRSC31415, DRSC31416
Tm1	FBgn0003721	DRSC13082, DRSC13083, DRSC16886, DRSC25249
up	FBgn0004169	DRSC20382, DRSC28798
mtm	FBgn0025742	DRSC03576, DRSC36585, DRSC36764, DRSC36765

Rya-r44F	FBgn0011286	DRSC07543
mew	FBgn0004456	DRSC18971, DRSC20352, DRSC35847
Mhc	FBgn0002741	DRSC03367, DRSC25959, DRSC34448, DRSC34449
up	FBgn0004169	DRSC20382, DRSC28798
sls	FBgn0003432	DRSC08528, DRSC08540, DRSC08670, DRSC32611, DRSC32612, DRSC36617, DRSC36618
sqh	FBgn0003514	DRSC18837, DRSC23800, DRSC34474, DRSC34475
mlc-c	FBgn0004687	DRSC18683, DRSC26543
wupA	FBgn0004028	DRSC20385, DRSC22547, DRSC29330, DRSC31986
bt	FBgn0005666	DRSC17129, DRSC17171, DRSC34355, DRSC34356, DRSC36656, DRSC36657
Vinc	FBgn0004397	DRSC18728, DRSC31286, DRSC31287
Rya-r44F	FBgn0011286	DRSC07543
tafazzin	FBgn0026619	DRSC07704, DRSC27100, DRSC36045
Dys	FBgn0024242	DRSC13360, DRSC13364, DRSC15260, DRSC16218, DRSC16219, DRSC16220, DRSC16232, DRSC16935
Lam	FBgn0002525	DRSC03359, DRSC33323, DRSC33324
mfr	FBgn0035935	DRSC10543
Scgdelta	FBgn0025391	DRSC18544
CalpB	FBgn0025866	DRSC11109, DRSC25885
Scgalpha	FBgn0032013	DRSC03076, DRSC29625
Scgdelta	FBgn0025391	DRSC18544
CG15105	FBgn0034412	DRSC05768, DRSC06532, DRSC27711
wb	FBgn0004002	DRSC03634, DRSC36402

Table S4. List of 1140 dsRNA amplicons screened in this study and their targeting genes

Amplicon	Gene
DRSC08557	CG2162
DRSC11227	Msr-110
DRSC08556	Sk2
DRSC10484	CG5146
DRSC08290	CG1271
DRSC10486	CG5150
DRSC08489	CG16753
DRSC09748	CG10591
DRSC08413	CG32486
DRSC09746	Sse
DRSC08190	CG11486
DRSC11145	DnaJ-1
DRSC08538	CG1869
DRSC11313	Ubp64E
DRSC08733	prominin-like
DRSC09745	CG10576
DRSC08200	CG11537
DRSC10509	CG5505
DRSC08298	CG1291
DRSC10512	CG32912
DRSC08415	CG14956
DRSC09742	CG10542
DRSC10949	CG8006
DRSC10683	CG32053
DRSC10952	CG8023
DRSC10681, DRSC34404	CG6640
DRSC09674	CG7207
DRSC10666	CG32055
DRSC10785	CG7197
DRSC10956	CG32063
DRSC10030	CG13671
DRSC11354	hay
DRSC10766	CG7066
DRSC11147	E(z)
DRSC10782	CG7188
DRSC10950	CG8009
DRSC10781	CG7185
DRSC10652	CG32066
DRSC10770	CG7081
DRSC10946	CG8003
DRSC10780	CG7182
DRSC10942	simj
DRSC10262	CG17352
DRSC10633	CG6418
DRSC08243	CG12079
DRSC10515	CG5537
DRSC08236	CG32281
DRSC10518	CG5568
DRSC08424	CG14965
DRSC09737	Pole2
DRSC08518	gry

DRSC09736	CG32412
DRSC08426	CG14967
DRSC09734	CG10483
DRSC08237	CG12034
DRSC09684	Bj1
DRSC08521	CG17746
DRSC09733	CG10479
DRSC08217	CG12009
DRSC10649	Jon65Aiii
DRSC08519	CG17723
DRSC09730	CG10472
DRSC08224	CG12016
DRSC09791	loj
DRSC08194	CG11526
DRSC10738	Ets65A
DRSC08221	PHGPx
DRSC11164	Ets65A
DRSC10779, DRSC34442, DRSC34441	Idh
DRSC10630	CG6409
DRSC10777	CG33057, mkg-p
DRSC09672	CG6404
DRSC10028	CG13667
DRSC10625	CG6327
DRSC10776	Oseg1
DRSC10926	CG7888
DRSC10322	mtrm
DRSC10623	CG6321
DRSC10763	CG32354
DRSC10621	CG32069
DRSC10761	CG7015
DRSC10921	CG7839
DRSC10757	CG6983
DRSC11200	JIL-1
DRSC10694	CG6683
DRSC09859	Mnf
DRSC10691	CG6673
DRSC10607	Ufd1-like
DRSC10292	CG32352
DRSC10893	CG7628
DRSC10608	CG32352
DRSC10605	MRP
DRSC08428	CG14969
DRSC09717	CG10289
DRSC08719	kst
DRSC10829	CG7376
DRSC08141	YT521-B
DRSC09716	CG10274
DRSC08653	CycJ
DRSC11133	D19A
DRSC08430	CG14971
DRSC11309, DRSC32777	Trn
DRSC08665	ImpE2
DRSC11207	LanA
DRSC08658	Eip63E
DRSC09715	CG10226

DRSC08156	CG10359
DRSC11277	SP1173
DRSC08169	CG32264
DRSC09699	CG32394
DRSC08166	CG10855
DRSC09698	CG10107
DRSC08165	CG32262
DRSC10992	CG8549
DRSC08216	CG12006
DRSC09697	CG10103
DRSC10565	CG5989
DRSC10603	GlcAT-P
DRSC10616	CG6282
DRSC10601	CG6199
DRSC10627	CG6372
DRSC10600	CG6190
DRSC10564	CG5978
DRSC09681	CG7600
DRSC10631	CG6416
DRSC10878	CG7557
DRSC10563	CG5971
DRSC11335	chrb
DRSC11353	h
DRSC09857	CG33047
DRSC11255, DRSC26929	Prm
DRSC09856	Mob1
DRSC10546	CG32030
DRSC10587	CG33490
DRSC10545	CG32030
DRSC10582	CG6091
DRSC11338	dally
DRSC10581	CG6084
DRSC11219	Mcm7
DRSC10822	CG7351
DRSC08698	Scsalpha
DRSC09696	CG32392
DRSC08158	CG1079
DRSC09692	Prat2
DRSC08162	Sc2
DRSC09691	CG10077
DRSC08145	CG10863
DRSC11104	CG9948
DRSC08207	CG11594
DRSC11394	Surf1
DRSC08180	CG1135
DRSC11168	G-ialpha65A
DRSC08184	CG1136
DRSC10193	CG33171
DRSC08711	dib
DRSC10194	CG14823
DRSC08741	wit
DRSC10297	form3
DRSC08451	Faa
DRSC11021	corn
DRSC08661	Gad1

DRSC11017	CG8616
DRSC08448	CG14989
DRSC11235	Neos
DRSC10542	CG5741
DRSC09853	CG11660
DRSC10540	CG5735
DRSC11303	TfIIEalpha
DRSC10467	mRpL12
DRSC10815	Sug
DRSC10470	CG5026
DRSC09851	CG11652
DRSC10475	CG5064
DRSC10809	CG7319
DRSC10500	CG5288
DRSC10573	CG6038
DRSC10476	CG5068
DRSC10808	Bmcp
DRSC11397	smg
DRSC10571	
DRSC10492	CG5194
DRSC10569	CG6004
DRSC10460	Argk
DRSC11253	Pi3K68D
DRSC10456	CG4911
DRSC11206	Klp68D
DRSC10462	CG4942
DRSC09847	CG11597
DRSC08452	CG14995
DRSC11015	mRpL50
DRSC08450, DRSC34432, DRSC34433	CG14991, Fit1
DRSC11112	Cdc27
DRSC08649	Chd64
DRSC11014	Trap36
DRSC08454	CG14998
DRSC11011	RhoGEF4
DRSC08691	RfC40
DRSC11010	CG8605
DRSC08693	Rop
DRSC11009	CG8602
DRSC08720	mas
DRSC11007	CG8600
DRSC08660	Ero1L
DRSC11006	eco
DRSC08204	VhaM9.7-1
DRSC11362	lark
DRSC08738	tipE
DRSC11005	CG8596
DRSC08666	ImpL2
DRSC11004	CTCF
DRSC08453	CG14997
DRSC11003	pst
DRSC10439	CG4641
DRSC11123	CycA
DRSC11264	Rdl
DRSC10539	CG5718

DRSC10411	UGP
DRSC10789	CG7252
DRSC10421	CG4447
DRSC10750	CG6931
DRSC10422	CG4452
DRSC10326	viaf
DRSC11192	CG32041
DRSC10537	CG5684
DRSC11189	Hsp26
DRSC10749	CG6928
DRSC11188	Hsp23
DRSC10715	l(3)j2D3
DRSC11190	Hsp27
DRSC10252	CG17153
DRSC10398	CG4080
DRSC09843	CG11560
DRSC11342, DRSC32113, DRSC32114	eIF-4E
DRSC09840	CG11534
DRSC10373	CG3672
DRSC10532	CG5645
DRSC08463	ago
DRSC11001	
DRSC08464	CG15011
DRSC11000	CG8580
DRSC08302	CG1309
DRSC10998	SMSr
DRSC08203	CG11586
DRSC10997	CG8564
DRSC08202	CG11583
DRSC10994	CG8560
DRSC08465	CG15012
DRSC10335	CG33277
DRSC08466	dyl
DRSC11131	Cyp4d8
DRSC08469	Cip4
DRSC10988	CG8539
DRSC08529	CG18314
DRSC10871	CG7546
DRSC08589	CG7447
DRSC11363	lqf
DRSC08591	Syx17
DRSC10867	CG7526
DRSC08178	CG11347
DRSC10860	CG7506
DRSC10374	CG3689
DRSC10717	RhoGAP68F
DRSC10392	CG3967
DRSC11238	Nrx
DRSC11320	aay
DRSC10529	Rh7
DRSC10369	CG3529
DRSC10528	thoc6
DRSC10367	phol
DRSC10412	CG4357
DRSC10365	CG3434

DRSC10293	CG32103
DRSC10371	CG32043
DRSC09750	CG10616
DRSC10330	CG32043
DRSC09768	CG10657
DRSC11314	Uch-L3
DRSC09777	CG10681
DRSC10372	CG3654
DRSC09779	CG10686
DRSC10364	CG3428
DRSC11248	Pcaf
DRSC10362	CG32036
DRSC09755	CG10627
DRSC08728	nAcRbeta-64B
DRSC10855	CG7492
DRSC08182	CG11353
DRSC09871	CG12262
DRSC08327	CG32245
DRSC11184	Hn
DRSC08696	Rpd3
DRSC10834	CG32369
DRSC08708	
DRSC11381	pbl
DRSC08535	CG18418
DRSC10963	syd
DRSC08318	Gef64C
DRSC11259	RNaseX25
DRSC08596	CG7509
DRSC09676	CG8042
DRSC08656	Dhc64C
DRSC10958, DRSC34409	CG8044
DRSC08595	Aats-leu
DRSC11377	nmo
DRSC08692	Rh50
DRSC11327	bip1
DRSC08652	Con
DRSC10881	CG7565
DRSC11273, DRSC32598	RpS9
DRSC09751	Tsf2
DRSC10352	CG3088
DRSC10396	CG4069
DRSC10357	CG3306
DRSC09758	CG10632
DRSC11208	LanB2
DRSC11203	Klc
DRSC10980	CG8336
DRSC09817	CG10984
DRSC10712	fry
DRSC09813	CG10973
DRSC10978	CG8329
DRSC09812	CG10971
DRSC10304	CG18180
DRSC09809	l(3)00305
DRSC10222	CG16719
DRSC10277	CG17667

DRSC11312	UbcD4
DRSC09801	CG10754
DRSC10705	CG6761
DRSC09807	CG10960
DRSC10302	CG18178
DRSC09821	CG11009
DRSC10433	CG4603
DRSC10929	Ect4
DRSC10436	CG4618
DRSC09677	CG7927
DRSC09773	CG10672
DRSC09669	Arp66B
DRSC09772	CG10671
DRSC11340	msk
DRSC09660	Aats-ala-m
DRSC10933	CG7942
DRSC09679	CG10670
DRSC10938	CdsA
DRSC09771	CG32423
DRSC10858	CG7498
DRSC10440	CG4669
DRSC10941	CG7979
DRSC11361	lama
DRSC10840	ERR
DRSC10447	CG4769
DRSC10943	CG7986
DRSC09763	Uev1A
DRSC10833	CG7387
DRSC09753	CG10625
DRSC10828	CG7375
DRSC10300	defl
DRSC09822	Ent3
DRSC09659	ATPsyn-b
DRSC09799	CG10752
DRSC10170	
DRSC09830	CG11261
DRSC10969	CG8177
DRSC09829	MICAL-like
DRSC10968	Ilp2
DRSC09827	CG11255
DRSC11113	Cdk8
DRSC11270, DRSC34294	RpS12
DRSC10699	CG6718
DRSC10278	RpS12
DRSC11298, DRSC33206	Taf2
DRSC11197	ImpL1
DRSC11109	CalpB
DRSC09711	CG10171
DRSC11231	Nc
DRSC09713	CG10191
DRSC10692	CG6674
DRSC09787	CG10724
DRSC09867	Ard1
DRSC09788	CG10725
DRSC09700	CG10116

DRSC10428	CG32158
DRSC09796	CG32130
DRSC11399	st
DRSC09687	bru-3
DRSC10407	CG4229
DRSC11033	CG8745
DRSC11223	Mipp1
DRSC11050	CG8833
DRSC11365	mbf1
DRSC11175	Gl
DRSC10403	nxf2
DRSC11052	CG9028
DRSC10223	Smn
DRSC11044	CG8783
DRSC09682	CG17286
DRSC11051	CG9007
DRSC11256, DRSC32168, DRSC32169	Pros26
DRSC10658	endos
DRSC11224	Mo25
DRSC10685	CG6650
DRSC11142	Dbp73D
DRSC11056	CG32210
DRSC11781	CG5656
DRSC11064	CG9300
DRSC11763	Syx7
DRSC11054	CG9231
DRSC11866	Hr78
DRSC11325	ash1
DRSC11835	CG7529
DRSC11299	Taf6
DRSC11815	CG33214
DRSC11067	CG9368
DRSC11836	CG7597
DRSC11049	CG8798
DRSC11840	CG7611
DRSC11047	CG8793
DRSC11812	CG7173
DRSC11324	asf1
DRSC11849	Smc5
DRSC11046, DRSC34110, DRSC34111	CG8789
DRSC11648	CG11307
DRSC11043	Oat
DRSC11647	CG11306
DRSC10687	CG6661
DRSC11093	CG9701
DRSC11186	Hsc70Cb
DRSC11237	Nrt
DRSC10638	blue
DRSC11094	CG9705
DRSC10721	CG6833
DRSC11095	CG9706
DRSC11358	l(3)70Da
DRSC11088	CG9674
DRSC10025	Sox21b
DRSC11099	CG9715

DRSC10914	CG7768
DRSC11396	Rh4, sina
DRSC10931	CG7924
DRSC11105	CG9951
DRSC10928	CG7906
DRSC09865	CG11915
DRSC10024	CG13482
DRSC09863	CG11905
DRSC10380	CG3868
DRSC11084	CG9665
DRSC11400	stwl
DRSC09854	Nc73EF
DRSC11174	Gbeta76C
DRSC11808	Trap220
DRSC11038	CG8756
DRSC11677	CG32444
DRSC11032, DRSC31589	CG8743
DRSC11806	CG7158
DRSC11180	
DRSC11644	CG11248
DRSC10987	CG8533
DRSC11732	CG32447
DRSC10104	CG14103
DRSC11643	CG11247
DRSC10218	CG15881
DRSC11642	Rpb8
DRSC11126	Cyp305a1
DRSC11823	
DRSC11031	Fibp
DRSC11824	CG7407
DRSC10983	kto
DRSC11825	CG7414
DRSC11246	Paps
DRSC11802	CG7148
DRSC11261	Rab8
DRSC11801	CG7145
DRSC10389	CG3919
DRSC09673	CG3799
DRSC11082	CG9628
DRSC10375	CG3764
DRSC11266	RecQ5
DRSC10690	CG6664
DRSC10281	dlp
DRSC10907	CG7728
DRSC10457	
DRSC10686	CG6652
DRSC10017	CG13473
DRSC10908, DRSC32125, DRSC32126	CG7729, Fit2
DRSC11308	Trl
DRSC10909	CG7730
DRSC11065	CG9311
DRSC10923	CG7842
DRSC10502	CG5295
DRSC10075	scaf6
DRSC11072	CG9425

DRSC10924	CG7853
DRSC10497	gnu
DRSC10906	rogdi
DRSC11306	Tom
DRSC10905	CG7724
DRSC10954	Su(Tpl)
DRSC11896	mub
DRSC11274, DRSC32192	Rpn1
DRSC11800	DNApol-eta
DRSC10947	CG8004
DRSC11828	CG7448
DRSC10919	RhoGDI
DRSC11831	CG7470
DRSC09662, DRSC32652	Ac76E
DRSC11611	CG7139
DRSC11346	fln
DRSC11798	CG7133
DRSC10899	Tom20
DRSC11607	CG9063
DRSC10901	CG7668
DRSC11862	Ddx1
DRSC10911	fat2
DRSC11669	CG11523
DRSC10182	CG14183
DRSC11860	Csp
DRSC10185	CG14186
DRSC11668	CG11489
DRSC10824	CG7365
DRSC11865	Hem
DRSC10482	CG5114
DRSC10657	CG6512
DRSC11257, DRSC32178, DRSC32179	Prosbeta2
DRSC10647	CG6479
DRSC10504	CG5392
DRSC10639	Mip
DRSC10700	cp309
DRSC11328	blot
DRSC10711	Aats-gly
DRSC10384	CG3885
DRSC10728	CG6854
DRSC10883	Oatp74D
DRSC10005	CG13458
DRSC10624	CG6322
DRSC10244	CG17081
DRSC10620	CG6311
DRSC10230	CG16959
DRSC11124	CycT
DRSC09879	CG12316
DRSC10613	Eip74EF
DRSC10731	CG6859
DRSC10861	CG7510
DRSC10735	CG6876
DRSC10857	CG7497
DRSC11351	gig
DRSC11667	Aats-ile

DRSC10756	CG6981
DRSC11661	CG11440
DRSC10802	CG7298
DRSC11794	CG6838
DRSC10751	CG6933
DRSC11894	mael
DRSC10250	CG17149
DRSC11652	CG32454
DRSC10259	CG17233
DRSC11641	CG11241
DRSC11116	Clc
DRSC11640	l(3)04053
DRSC10323	CG32226
DRSC11822	CG7369
DRSC11384, DRSC34463	polo
DRSC11889	jim
DRSC11285	Snap
DRSC11851	CG32462
DRSC10693	CG6680
DRSC11606	Arf79F
DRSC11779	eRF1
DRSC11633	CG11109
DRSC10760	CG7011, CG6876
DRSC11252	Pep
DRSC10790	CG7255
DRSC11201	CG32177
DRSC10918	ran-like
DRSC10062	Ccn
DRSC10796	CG7275
DRSC10566	Adgf-A
DRSC10934	CG7945
DRSC10523	CG5589
DRSC11122	CrebA
DRSC10519	CG5577
DRSC10847	AGO2
DRSC10517	CG5567
DRSC10655	CG6498
DRSC10516	CG5546
DRSC10231	CG16979
DRSC10845	CG7430
DRSC10913	Tfb2
DRSC10848	CG7441
DRSC09875	CG12301
DRSC10514	CG5535
DRSC09877	CG12304
DRSC10501	CG5290
DRSC11780	CG5618
DRSC11630	Chro
DRSC11610	DNAprim
DRSC11634	Ssl1
DRSC11867	Ide
DRSC11635	slif
DRSC11877	RhoBTB
DRSC11637	CG11133
DRSC11608	CG5498

DRSC11632	Mes2
DRSC11775	CG5282
DRSC11917	alpha-Cat
DRSC11774	CG5274
DRSC11933	
DRSC11773	CG5262
DRSC12206	CG12581
DRSC11772	Las
DRSC12208	CG12582
DRSC11771	mRpL15
DRSC12161	auxillin
DRSC11670	CG11796
DRSC12288	CG18143
DRSC11787	CG5932
DRSC12227	CG14641
DRSC10900	CG7656
DRSC11161	Eip75B
DRSC10232	RhoGAP71E
DRSC10047	CG13698
DRSC10827	CG7372
DRSC10485	CG5147
DRSC10594	CG6151
DRSC10818	CG7341
DRSC10597	CG6169
DRSC10807	CheA75a
DRSC09900	CG12713
DRSC09988	CG13380
DRSC10590	CG6114
DRSC11378	not
DRSC10243	GXIVsPLA2
DRSC10744	CG6897
DRSC10242	CG17033
DRSC10743	CG6896
DRSC10559, DRSC32419	CG5931
DRSC10404	GNBP2
DRSC10238	CG17027
DRSC10401	Chmp1
DRSC10570	CG6017
DRSC11125	Cyp12c1
DRSC11788	CG5955
DRSC12372, DRSC31883	abs
DRSC11697	CG32428
DRSC12350	Gel
DRSC11789	CG5969
DRSC12228	CG14642
DRSC11791, DRSC34398	CG6020
DRSC12225	CG14639
DRSC11742	CG18281
DRSC12151	CG1092
DRSC11764	CG32425
DRSC12333	CG9780
DRSC11759	CG5047
DRSC12124	CG1102
DRSC11892	knrl
DRSC12332, DRSC34417	CG9779

DRSC11874	Pitslre
DRSC12335	CG9791
DRSC11750	CG3947
DRSC12336	CG9795
DRSC11655	CG11399
DRSC12127, DRSC34416	CG9776
DRSC11749	CG3698
DRSC12329	CG9772
DRSC10556	mRpS31
DRSC10397	Nufip
DRSC11404	th
DRSC10736	Aut1
DRSC10525	Mbs
DRSC10734	l(3)neo26
DRSC10495	CG5241
DRSC10393	Indy
DRSC10499	CG5284
DRSC11263	Rad9
DRSC10493	CG5222
DRSC11315	Ugt
DRSC11318	Zn72D
DRSC10390	CG3961
DRSC11297, DRSC31762	Taf4
DRSC10386	CG3893
DRSC10490	Pgm
DRSC11108	CSN1b
DRSC11290	SsRbeta
DRSC10724	CG6841
DRSC10229	CG16838
DRSC10723	CG6839
DRSC10468	CG5018
DRSC10722	CG6836
DRSC11755	CG4365
DRSC12160	CG1103, CG9772
DRSC11748	CG3680
DRSC12150	CG1090
DRSC11746	CG3618
DRSC12149	Cont
DRSC11875	Pka-R1
DRSC12389	tub
DRSC11674	CG12452
DRSC12232	CG14646
DRSC11665	CG11456
DRSC12344	CG9855
DRSC11887	fng
DRSC12343	CG9853
DRSC11625	CG10585
DRSC12233	CG14647
DRSC11621	CG10566
DRSC12234, DRSC34034	CG14648
DRSC11620	CG10565
DRSC12143	CG1074
DRSC11618	park
DRSC12338	CG9804
DRSC11617	park

DRSC12236	CG14650
DRSC10471, DRSC34390	CG5027
DRSC10295	CG18135
DRSC10459	CG4925
DRSC10084	Mkp3
DRSC11249	Pdh
DRSC10720	MESR6
DRSC10451	CG4818
DRSC09845	CG11577
DRSC10449	CG4784
DRSC09722	CG10424
DRSC10227	CG16807
DRSC09721	CG10419
DRSC10445	CG4729
DRSC10087	fz2
DRSC10443	CG4877
DRSC11218	Max
DRSC10441	CG4680
DRSC11085	CG9666
DRSC11345	fax
DRSC11083	CG9629
DRSC11296	TMS1
DRSC11081	CG9619
DRSC10430	Aats-tyr
DRSC11087	fal
DRSC11614	CG10510
DRSC12337, DRSC34377	CG31523
DRSC11612	CG10508
DRSC12147	CG1078
DRSC11857	CG9389
DRSC11990	5-HT2
DRSC11603	AcCoAS
DRSC12330	CG9775
DRSC11899	ppl
DRSC12142	Trap18
DRSC11848	Z4
DRSC12386	rpk
DRSC11650	CG11309
DRSC12355	Karybeta3
DRSC11837	Rab26
DRSC12139	CG31531
DRSC11821	CG7338
DRSC12141	CG31534
DRSC11820	CG7324
DRSC12126	Nep2
DRSC11609, DRSC34396	CG6014
DRSC12388	tacc
DRSC11792	CG6049
DRSC12310, DRSC34353	atms
DRSC14140	Aats-gln
DRSC14133	CG14526
DRSC14248	CG10513
DRSC16650	Doa
DRSC14428	CG11892
DRSC14873	CG14521

DRSC14251	CG10550
DRSC15403	CG1951
DRSC14257	CG10562
DRSC14146	CG1957
DRSC14262	CG10675
DRSC16791	Pkc98E
DRSC17044	rha
DRSC14397	CG11837
DRSC16676	Fur1
DRSC14399	CG11841
DRSC14438	
DRSC14400	CG11842
DRSC15722	CG5127
DRSC14294	Sirt7
DRSC15594	XNP
DRSC14418	CG11874
DRSC15036, DRSC34369	CG1544
DRSC18494	CG11448
DRSC16925	chp
DRSC17952	
DRSC15035	CG1542
DRSC18604	CG14785
DRSC15236	CG1746
DRSC18605	CG14786
DRSC14467	CG12054
DRSC18607	l(1)G0431
DRSC15240	CG1750
DRSC18608	O-fut2
DRSC14475	CG12114
DRSC18565	pck
DRSC15130	CG1607
DRSC18567	Rab27
DRSC16678	Gcn2
DRSC18568	CG14782
DRSC14304	CG11337
DRSC18512	CG32810
DRSC16682	Gprk2
DRSC17788	CG11509
DRSC15718	CG5112
DRSC14420	CG11876
DRSC15716	CG5107
DRSC14421	CG11877
DRSC15615	CG4673
DRSC14423	CG11880
DRSC15621	CG4685
DRSC14424	CG11881
DRSC15707	CG5053
DRSC14148	Vha100-1
DRSC15655	LpR2
DRSC16787	Pglym78
DRSC15665	LpR1
DRSC16839, DRSC32198	Rpn2
DRSC15908	CG5886
DRSC14431	CG11897
DRSC14147	Tsp96F

DRSC14866	CG14507, CG14514
DRSC16729	Lnk
DRSC14155	CG15817
DRSC16758, DRSC34356	Nf1
DRSC14443	CG31445
DRSC16697	HLHmbeta
DRSC17071	stg
DRSC14468	CG12063
DRSC18765	dor
DRSC14322, DRSC33088	pygo
DRSC18507	CG32809
DRSC15131	CG1635
DRSC18592	CG32809
DRSC15258	CG1774
DRSC18733	a6
DRSC14324	CycG
DRSC18593	CG3795
DRSC15295	CG1800
DRSC17958	CG14801
DRSC15310	CG1815
DRSC18760, DRSC31062	deltaCOP
DRSC15434	CstF-50
DRSC18553	CG14814
DRSC15395, DRSC29064	CG1890
DRSC18551	CG14816
DRSC15397	CG1896
DRSC18555	CG14804
DRSC15432	l(3)s1921
DRSC18845	trr
DRSC15400	CG1910
DRSC18550	mRpL16
DRSC16962	gro
DRSC15439	CG2321
DRSC14886	CG14542
DRSC15412	CG2006
DRSC16643	Dak1
DRSC15413	CG2010
DRSC14898	CG31324
DRSC15437	Trc8
DRSC15962	CG6073
DRSC17002	Dr
DRSC14497	CG12290
DRSC15398	CG1906
DRSC14109	Ald
DRSC15399	CG1907
DRSC15981	CG31085
DRSC14168	Bub3
DRSC16931	dei
DRSC15401	CAP-D2
DRSC15805	CG5455
DRSC16690	Gycalpha99B
DRSC16054	CG6490
DRSC14131	CG7601
DRSC15809	CG5467
DRSC16266	CG7598

DRSC15427	CG2196
DRSC18738	arm
DRSC15419	CG2135
DRSC17963	CG32803
DRSC15402	sip3
DRSC18573	CG3810
DRSC15417	CG2118
DRSC18769	eIF2B-epsilon
DRSC14101	Acf1
DRSC18576	CG3573
DRSC15406	CG1971
DRSC18540	CG11596
DRSC16948	ferrochelatase
DRSC18542	CG3857
DRSC15409, DRSC34466	RhoGAP100F
DRSC18541	CG3587
DRSC16999	mod
DRSC17724, DRSC34351	Actn
DRSC16732	Map205
DRSC18514	CG4313
DRSC17176	pan
DRSC18521	CG4281
DRSC17127	Ank
DRSC18519	CG4199
DRSC16042	CG6447
DRSC15405	CG1969
DRSC16038	CG6425
DRSC14151	CG7609
DRSC16885	Tl
DRSC15407	CG1972
DRSC16702	His2Av
DRSC16977	kay
DRSC14136	sda
DRSC16325	CG7837
DRSC16022	CG6330
DRSC16715	Ice
DRSC16019	Tsp97E
DRSC16324	CG7834
DRSC16013	CG6296
DRSC16312	CG7789
DRSC16006	CG6271
DRSC17012	ncd
DRSC16757	NepYr
DRSC15305	CG31037
DRSC16004	Nep5
DRSC16316	CG7802
DRSC17065	spz
DRSC15052	CG31033
DRSC17157	CG2316
DRSC18520	CG4194
DRSC17137	CG31998
DRSC18517	CG4061
DRSC17163	Crk
DRSC18518	CG4045
DRSC17167	Rad23

DRSC18577	CG3835
DRSC17154, DRSC34373, DRSC34374	Ac76E
DRSC18697	Pgd
DRSC17143	Hcf
DRSC18851	wapl
DRSC17128	CG2052
DRSC18499	CG3630
DRSC17152	lgs
DRSC18458	Cyp4d2
DRSC17162	CaMKI
DRSC18455	Cyp4ae1
DRSC17170	bip2
DRSC18822	pn
DRSC17178	zfh2
DRSC18687	Nmd3
DRSC17166	Pur-alpha
DRSC18509, DSC34386	CG3457
DRSC15961	CG6070
DRSC16317	Cad99C
DRSC15906	CG5880
DRSC15301	CG18041
DRSC15958	CG6059
DRSC15053	CG15514
DRSC15956	CG6051
DRSC16320	CG7816
DRSC15939	CG31063
DRSC16319	CG7814
DRSC15936	CG18766
DRSC15051	CG31038
DRSC17026	pll
DRSC15058	capa
DRSC16882	TfIIA-L
DRSC16329	CG7866
DRSC15928	woc
DRSC16332	eIF2B-alpha
DRSC16983	l(3)mbt
DRSC16335	CG7896
DRSC15923	CG5938
DRSC14318	CG11504
DRSC15485	CG3368
DRSC16340	Tace
DRSC17150	CG1909
DRSC18728, DRSC32186	Vinc
DRSC17135	CG31992
DRSC18816	pcx
DRSC17146	Slip1
DRSC18775	fs(1)K10
DRSC17174	myoglianin
DRSC18755, DRSC31852	crn
DRSC17129, DRSC34355, DRSC34356	bt
DRSC18530	CG3191
DRSC17171	bt
DRSC18531	CG3078
DRSC17148	Arc70

DRSC18271	l(1)G0144
DRSC17205	CG11155
DRSC18526	CG3071
DRSC17196	cals
DRSC18525	CG2924
DRSC17216	RfaBp
DRSC18524	CG2918
DRSC17214	CaMKII
DRSC18527	CG2865
DRSC17220	plexA
DRSC18855	z
DRSC15481	bigmax
DRSC16759	Nlp
DRSC15477	CG3330
DRSC16346	CG7920
DRSC15853	CG5646
DRSC16347, DRSC34446	Mgat2
DRSC15850	dsd
DRSC14120	Axn
DRSC14161	RpS10a
DRSC16349	CG7928
DRSC15839	CG5590
DRSC16868	Sry-beta
DRSC16825	Sce
DRSC16869	Sry-delta
DRSC14568	CG12880
DRSC16351	CG7943
DRSC14564	CG12876
DRSC16352	CG7946
DRSC14566	btz
DRSC16353	CG7950
DRSC14518	CG12428
DRSC15421	CG31025
DRSC15694	CG5003
DRSC16888	Tpi
DRSC17222	toy
DRSC18676	Klp3A
DRSC17201	CG32016
DRSC18793	mit(1)15
DRSC17218	eIF-4G
DRSC18427, DRSC32087	CG8636
DRSC17223	unc-13
DRSC18501	CG2652
DRSC17202	CG11148
DRSC18464	CG2681
DRSC17204	Sox102F
DRSC18470	CG2694
DRSC18752	cin
DRSC18590	CG2701
DRSC18459	Cyp4g1
DRSC18776	fs(1)Ya
DRSC18787	Exp6
DRSC18766	dwg
DRSC18288	CG18166, CG3176, CG32817
DRSC18587	CG2713

DRSC18505	CG18273
DRSC18589	CG2712
DRSC18503	CG3156
DRSC18754	crm
DRSC14488	mRpS22
DRSC16741, DRSC32500, DRSC32501	Mlc2
DRSC14487	CG33213
DRSC16554	CG9747
DRSC15693	CG4980
DRSC16536	CG9682
DRSC16833, DRSC32560	RpL4
DRSC16671	Fer1HCH
DRSC14132	CG5508
DRSC14141	CG2217
DRSC15824	CG5514
DRSC15428	CG2218
DRSC15827	Gp93
DRSC16901	aralar1
DRSC15682	CG4951
DRSC14932	CDase
DRSC14925	CG31374
DRSC14473	PH4alphaEFB
DRSC16749	Mst98Ca
DRSC16546, DRSC34461	PH4alphaNE1
DRSC14598	Gfat2
DRSC16975	jdp
DRSC15364	Moca-cyp
DRSC17062, DRSC34480, DRSC34481	spdo
DRSC18502	CG17896
DRSC17764	CG10804
DRSC18737	arg
DRSC17762	CG10802
DRSC18772	elav
DRSC17763	CG10803
DRSC18557	CG4293
DRSC18231	CG2875
DRSC17728	Appl
DRSC18696	Parg
DRSC18487	CG13366
DRSC17894	Mnt
DRSC18788	l(1)1Bi
DRSC18245	CG32789, CG2947
DRSC18461	Dredd
DRSC18854	yin
DRSC18482	Suv4-20
DRSC17730	CG2930
DRSC18833	skpA
DRSC18242	VhaAC39
DRSC18831	sdk
DRSC18243	CG2938
DRSC18537	Pomt2
DRSC18384	Vap-33-1
DRSC15034	CG31051
DRSC15433	CG2246
DRSC16761	Noa36

DRSC16541	PH4alphaNE3
DRSC16709	Hrb98DE
DRSC14596	CG1342
DRSC16586	CG9986
DRSC14582	CG1340
DRSC14174	CG10011
DRSC17098	zfh1
DRSC16589	CG9990
DRSC14126	CG31012
DRSC14528	CG12558
DRSC16849	Sap-r
DRSC17095	wdn
DRSC16631	Cyp4c3
DRSC15133	CG1646
DRSC12635	5-HT7
DRSC15033	CG1523
DRSC16929	dco
DRSC15134	CG1647
DRSC14299	CG11317
DRSC14857	inx3
DRSC16691	Gycbeta100B
DRSC18536	CG13360
DRSC18403, DSC31278	lva
DRSC18704	Rbf
DRSC18746	brn
DRSC18538	CG7359
DRSC18662	CG6133
DRSC17747	CDC45L
DRSC18661	CG6121
DRSC18840	su(w<u*P*>a</u*P*>)
DRSC18664	Fas2
DRSC18532	CG11403
DRSC18252	CG2982
DRSC18579	CG11409
DRSC18806	norpA
DRSC18583	CG11412
DRSC18309	CG3556
DRSC18580	CG12773
DRSC18310	CG3564
DRSC18581	CG11417
DRSC17783	CG11436
DRSC18492	CG3056
DRSC17784	CG11444
DRSC18714	SNF1A
DRSC18559	CG12179, CG12184

Additional information on the specific genes can be obtained at http://flyrnai.org/.